Disentangling between tectonic, eustatic and sediment flux controls on the 20 Ma-old Burdigalian transgression of the Molasse basin in Switzerland

Philippos Garefalakis[1], Fritz Schlunegger[1]

[1]Institute of Geological Sciences, University of Bern, Bern, CH-3012, Switzerland

Correspondence to: Philippos Garefalakis (philippos.garefalakis@geo.unibe.ch)

Abstract

The stratigraphic architecture of the Swiss Molasse basin, situated on the northern side of the evolving Alps, reveals crucial information about the basin's geometry, its evolution and the processes leading to the deposition of the siliciclastic sediments. Nevertheless, the formation of the Upper Marine Molasse and the controls on the related Burdigalian transgression have still been a matter of scientific debate. During the time period from c. 20 to 17 Ma, the Swiss Molasse basin was partly flooded by a shallow marine sea, striking SW – NE. We conducted sedimentological and stratigraphic analyses of several sites across the entire Swiss Molasse basin. An attempt is made to extract stratigraphic signals that can be related to changes in sediment supply rate, variations in the eustatic sea level and subduction tectonics.

Field investigations show that the transgression and the subsequent evolution of the Burdigalian seaway was characterized by (i) changes in sediment transport directions, (ii) a deepening and widening of the basin, and (iii) phases of erosion and non-deposition. We use these changes in the stratigraphic record to disentangle between tectonic and surface controls at various scales. As the most important mechanism, roll-back subduction of the European mantle lithosphere and delamination of crustal material most likely explain the widening of the Molasse basin particularly at distal sites. In addition, delamination of crustal material also caused uplift of the Aar-massif. This process was likely to have shifted the patterns of surface loads. Such mechanisms could have caused a flexural adjustment of the foreland plate beneath the Molasse basin, which we use as mechanism to explain the establishment of distinct depositional environments and particularly the formation of subtidal-shoals where a bulge is expected. In the Alpine hinterland, roll-back subduction occurred simultaneously with a period of rapid tectonic exhumation accomplished through slip along the Simplon detachment fault and a change in the organization of the drainage network, with the consequence that the sediment flux to the basin decreased. It is possible that this reduction in sediment supply contributed to the establishment of marine conditions in the Swiss Molasse basin and thus amplified the effect related to the tectonically controlled widening of the basin. Because of the formation of shallow marine conditions, subtle changes in eustatic sea level contributed to the occurrence of several hiatuses that chronicle periods of erosion and non-sedimentation. Whereas these mechanisms are capable of explaining the establishment of the Burdigalian seaway and the formation of distinct sedimentological niches in the Swiss Molasse basin, the drainage reversal during OMM-times possibly

requires a change in tectonic processes at the slab scale, possibly including the entire Alpine range between the Eastern and Central Alps. In conclusion, we consider roll-back tectonics as the main driving force controlling the transgression of the OMM in Switzerland, with contributions by uplift of individual crustal blocks (here the Aar-massif), all of which are related to the subduction processes. In addition, the reduction of sediment flux was likely to have been controlled by tectonic processes as well when the basement blocks became uplifted and when slip along detachment faults in the core of the Alps changed the catchment geometries. Eustatic changes in sea level possibly explain the various hiatuses.

1 Introduction

Foreland basins and their deposits have often been used for exploring the tectonic evolution of their hinterlands, mainly because these basins are mechanically coupled with the adjacent mountain belts (Beaumont, 1981; Jordan, 1981; DeCelles, 2004). The formation of these foreland basins occurs through the flexural downwarping of the underlying lithosphere in response to loading, which results in the formation of a wedge-shaped trough where sediment accumulates (DeCelles and Giles, 1996; Allen and Allen, 2005). The shape of the foreland trough depends on the mechanical properties of the foreland plate (Sinclair et al., 1991; Flemings and Jordan, 1990; Jordan and Flemings, 1991), on the load of the sedimentary fill itself (Flemings and Jordan, 1990; Jordan and Flemings, 1991), and predominantly on the tectonic and geodynamic processes leading to changes in plate loading (Beaumont, 1981; Jordan, 1981; Allen et al., 1991; Sinclair et al., 1991; DeCelles and Gilles, 1996). This is particularly the case for the North Alpine Foreland Basin, or the Molasse basin, situated on the northern side of the European Alps (Fig. 1a), which has been investigated in detail over the past decades with a focus on relating changes in the basin's evolution to Alpine orogenic events (e.g. Pfiffner, 1986; Schlunegger et al., 1997a; Kempf et al., 1999; Kuhlemann and Kempf, 2002; Ortner et al., 2011). In the Swiss part, this basin has experienced two periods when sedimentation occurred within a sea (Matter et al., 1980). The Burdigalian time (early Miocene), c. 20 Ma ago, was such a period when the basin became occupied by a shallow-marine seaway, linking the Paratethys in the NE with the Tethys in the SW (Allen et al., 1985). The marine ingression resulted in the accumulation of marine sediments, which have been referred to as Upper Marine Molasse group (OMM; Matter et al., 1980; Allen, 1984). Although the history and geometry of the Burdigalian seaway and the related sedimentary processes are well known through detailed sedimentological and chronological investigations (e.g. Lemcke et al., 1953; Allen, 1984; Allen et al. 1985; Homewood et al. 1986; Doppler, 1989; Keller, 1989; Jin et al., 1995; Salvermoser, 1999; Strunck and Matter, 2002; Kuhlemann and Kempf, 2002; Reichenbacher et al., 2013), the controls on this transgression have still been a matter of ongoing scientific debate. Previous authors (e.g. Allen et al., 1985; Homewood et al., 1986; Keller, 1989; Strunck and Matter, 2002; Reichenbacher et al., 2013) proposed a combination of a reduced sediment flux and a rise in global sea level as possible mechanisms. However, thermo-chronometric data from the core of the Alps (Lepontine dome, Fig. 1; Boston et al., 2017) and structural work in the external Aar-massif (Fig. 1; Herwegh et al., 2017) revealed that the Burdigalian was also the time of major thrusting, tectonic exhumation and surface loading in the Alps. These processes were related to the subduction of the European continental plate underneath the African plate (Schmid et al., 1996). Accordingly, it was proposed that tectonic processes were equally important to have caused a flexural downwarping of the foreland plate (Pfiffner et al., 2002; Schlunegger and Kissling, 2015) and, as a consequence, the transgression of the peripheral sea (Sinclair et al., 1991). The key to disentangle between these underlying mechanisms (eustacy, sediment flux, tectonics) is likely to be situated in the Swiss part of the Molasse basin, where the marine transgression resulted in the final connection, and thus in the linkage, of the Tethys in the SW with the Paratethys in the NE (Allen and Homewood, 1984).

The aim of this paper is to disentangle between tectonic processes, a reduction of sediment flux and changes in the eustatic sea level as controls on the transgression of the OMM in Switzerland. We analyzed OMM outcrops and sections along the entire Swiss Molasse basin at both proximal and distal positions relative to the Alpine front (Fig. 1a). To this extent, we investigated

palaeo-flow directions, sedimentary facies, and related depositional settings of the OMM, and we calculated palaeo-water depths using hydrological concepts. However, a chronological framework is absolutely required for correlating sections across a basin where facies relationships are strongly heterochronous, as it is the case for the Swiss Molasse basin (Matter et al., 1980). Therefore, we also re-assessed the temporal framework of the analysed sections through a compilation of previously published magnetostratigraphic and biostratigraphic data, and we correlated the individual sections across the basin.

2 Setting

2.1 The central European Alps and the Swiss Molasse basin

The architecture and evolution of the Alps

The doubly-vergent Alpine orogen (Fig. 1) is the consequence of the late Cretaceous to present continent-continent collision between the European and Adriatic plates (Schmid et al., 1996; Handy et al., 2010). It comprises a nappe stack with a crystalline core that is exposed in the Lepontine dome and the external massifs (e.g. Aar-massif; Spicher, 1980). At deeper crustal levels, the Alpine orogen is underlain by a thick crustal root made up of a stack of lower crustal material derived from the European continental plate (Fry et al., 2010; Fig. 1b). Beneath the core of the orogen, the c. 160 km-long (Lippitsch et al., 2003) lithospheric slab of the European continental plate bends the foreland plate towards the south-east, resulting in a downwarping of the European plate (Fig. 1b). This bending was mainly driven by slab loads due to the relatively large density of the subducted lithospheric mantle in comparison with the surrounding asthenosphere as seismo-tomography data reveals (Lippitsch et al., 2003). On the northern side of the orogen, the highest unit is made up of Austroalpine nappes that structurally overlie the (meta)sedimentary successions of the Penninic and the underlying Helvetic thrust nappes (Fig. 1a). The front of the Helvetic and Penninic units is referred to as the basal Alpine thrust (Fig. 1b). The southern side of the Alps is made up of the Southalpine thrust sheets that consist of crystalline basement rocks and sedimentary units of African origin. This fold-and-thrust belt is bordered to the south by the Po Basin (Fig. 1a). The north-vergent Alpine thrusts are separated from the South Alpine nappes by the north-dipping Periadriatic line that accommodated most of the shortening during the Oligocene and the early Miocene by backthrusting and right-lateral slip (Schmid et al., 1996). The Lepontine dome (Fig. 1), made up of Penninic crystalline rocks, is bordered to the west by the Simplon detachment fault, where normal faulting resulted in rapid tectonic exhumation of the dome between late Oligocene and early Miocene times with a peak recorded by thermo-chronometric data at 20 Ma (Fig. 1b; Hurford, 1986; Mancktelow, 1985; Mancktelow and Grasemann, 1997; Schlunegger and Willett, 1999; Boston et al., 2017). This was also the time, when the Aar-massif, situated on the European continental plate (Fig. 1b), experienced a period of rapid vertical extrusion (Herwegh et al., 2017).

Recently, slab loads have been considered as the major driving force of the subduction history of the European plate and for the exhumation of crystalline rocks (Kissling and Schlunegger, 2018). This also concerns the uplift of the Aar-massif and the rapid exhumation of the Lepontine dome (Fig. 1). Herwegh et al. (2017) and Kissling and Schlunegger (2018) proposed a mechanism referred to as roll-back subduction to explain these observations. According to these authors, delamination of crustal material from the European mantle lithosphere along the Moho resulted in a stacking of buoyant lower crustal rocks

beneath the Lepontine dome and the Aar-massif forming the crustal root (Fry et al., 2010; Fig. 1b). These processes are considered to have maintained isostatic equilibrium between the crust and the subducted lithospheric mantle and thus the elevated topography (Schlunegger and Kissling, 2015). Additionally, they most likely balanced, through the stacking of the crustal root (Fry et al., 2010, Fig. 1b), the rapid removal of upper crustal material in the Lepontine dome at c. 20 Ma (Schlunegger and Willet, 1999; Boston et al., 2017). Delamination of crustal material has also been invoked to explain the contemporaneous rapid exhumation and northward thrusting of the Aar-massif along steeply dipping thrusts (Herwegh et al., 2017). These processes occurred at the same time when (i) the drainage network of the Central Alps was reorganized (Kuhlemann et al., 2001a; Schlunegger et al., 1998), (ii) sediment flux to the basin decreased, as revealed by sediment budgets (Kuhlemann, 2000; Kuhlemann et al., 2001a, 2001b), and (iii) when the Burdigalian transgression occurred in the Swiss part of the Molasse basin. We will thus refer to these processes when discussing the controls on the Burdigalian transgression within a geodynamic framework.

The architecture and evolution of the Molasse basin

The approximately 700 km long and ENE – WSW striking basin stretches from France to Austria, where it broadens from <30 km to a maximum width of c. 150 km (Pfiffner, 1986; Fig. 1a). The Molasse basin is limited to the north by the Jura Mountains and the Black-Forest- and Bohemian-massifs, and to the south by the basal Alpine thrust (Homewood et al., 1986).

Reconstructions of the evolution of the Molasse basin (Fig. 2a) have been the focus of many research articles over the past years (e.g. Matter et al., 1980; Homewood and Allen, 1981; Allen, 1984; Keller, 1989; Schlunegger et al., 1996; Sinclair, 1997; Kempf et al., 1999; Kuhlemann and Kempf, 2002; Ortner et al., 2011; Reichenbacher et al., 2013). This has resulted in the general notion that the large-scale subsidence history of the Molasse basin was closely linked with the geodynamic evolution of the Alps (Sinclair et al., 1991; Kuhlemann and Kempf, 2002; Pfiffner et al., 2002; Ortner et al., 2011; Schlunegger and Kissling, 2015). The development of this basin as a foreland through has been considered to commence with the closure of the Alpine Tethys in late Cretaceous times (Lihou and Allen, 1996; Schmid et al., 1996). This was the time when subduction of the European oceanic lithosphere with a large density beneath the Adriatic continental plate started. Large slab load forces resulted in a downwarping of the European foreland plate and the formation of a deep marine trough (Schmid et al., 1996), where sedimentation occurred by turbidites (Sinclair, 1997). This resulted in the accumulation of mud- and sandstones on submarine fans (Allen et al. 1991; Lu et al., 2018). The material sources of these mass movements were situated in a volcanic arc on the African continental plate that represented the upper plate (Lu et al., 2018; Reichenwallner, 2019). This first period of basin evolution has been referred to as the underfilled or the Flysch stage in the literature (Fig. 2b; Sinclair and Allen, 1992), mainly because sedimentation occurred within a deep marine trough. The related deposits have been called the North Helvetic Flysch in the Alpine literature (NHF, early Oligocene; Sinclair and Allen, 1992). The situation changed at 35 – 32 Ma when the buoyant continental lithosphere of the European plate started to enter the subduction channel. Strong tension forces started to operate at the stretched margin of the European continental crust particularly beneath the Central Alps (Schmid et al., 1996), with the result that the subducted oceanic lithosphere of the European plate broke off (Davies and von Blanckenburg, 1995).

The consequence was a rebound of the European plate, a rise of the Central Swiss Alps and an increase in sediment flux to the Swiss Molasse basin (Sinclair, 1997; Kuhlemann et al., 2001a, 2001b; Willett, 2010; Garefalakis and Schlunegger, 2018), which became overfilled at c. 30 Ma (Sinclar and Allen, 1992; Sinclair, 1997). The subsequent post 30 Ma-stage of basin evolution has been referred to as the Molasse, or overfilled stage (Sinclair and Allen, 1992) (Sinclair, 1997). Molasse sedimentation occurred from c. 30 Ma onward and was recorded by two large-scale, transgressive-regressive mega-sequences (Fig. 2b; e.g. Sinclair, 1997; Kempf et al., 1997; 1999; Kuhlemann and Kempf, 2002; Cederbom et al., 2004; 2011). These two mega-sequences consist of four lithostratigraphic groups. The first mega-sequence comprises the Lower Marine Molasse (UMM; Diem, 1986) and the Lower Freshwater Molasse (USM; Platt and Keller, 1992), and the second mega-sequence consists of the Upper Marine Molasse (OMM; Homewood et al., 1986) and the Upper Freshwater Molasse (OSM; Matter et al., 1980). Sedimentation in the Molasse basin continued up to c. 10 – 5 Ma, when a phase of uplift during Pliocene times resulted in erosion and recycling of the previously deposited Molasse units (Mazurek et al., 2006: Cederbom et al., 2004; 2011). This erosion reached deeper stratigraphic levels in the western part of the Molasse basin than in the eastern segment (Baran et al., 2014) with the consequence that the OMM deposits are only fragmentarily preserved in the west (Fig. 2a).

Sediment dispersal has changed during the Molasse stage of basin evolution. Prior to 20 Ma, during USM times, measurements of sediment transport directions (Kempf et al., 1999) and sediment provenance tracing (Füchtbauer; 1964) revealed that the sedimentary material was transported to the east by braided to meandering streams. At that time, a coastline was situated near Munich, separating a deep marine trough farther east from a terrestrial environment to the west of Munich (Kuhlemann and Kempf, 2002). During OMM times, heavy mineral assemblages reveal that the Swiss Molasse basin operated as a closed sedimentary trough, where all supplied material was locally stored (Allen et al., 1985). During OSM times, heavy mineral data imply that material with sources in the Hercynian basement north of Munich or the Bohemian-massif was supplied to the Swiss Molasse ("Graupensandrinne"; Allen et al., 1985; Berger et al., 2005), suggesting that material transport occurred towards the west (Kuhlemann and Kempf, 2002). The details of the reversal of the drainage direction have not yet been elaborated, and related scenarios lack a database with palaeo-flow information, particularly for the OMM. The establishment of such a database will be part of the scope of this article, mainly because the reversal of drainage direction in the basin occurred sometime during deposition of the OMM.

2.3 The Upper Marine Molasse

Lithostratigraphic and sedimentologic framework

The Upper Marine Molasse (OMM) deposits, which are the focus of this study, mainly consist of a suite of shallow marine sandstones and mudstones that were deposited between c. 20 – 17 Ma (Fig. 2) in a c. 70 – 80 km-wide seaway (Allen and Homewood, 1984; Allen et al., 1985; Keller, 1989; Strunck and Matter, 2002). Close to the Alpine thrust front, the OMM-successions are up to 900 m thick and thin to a few tens of meters towards the distal basin margin farther northwest.

Large streams with sources in the Central Alps supplied their material to the Molasse basin, thereby forming megafans with diameters >10 km that interfingered with the sea (Schlunegger et al., 1996; Kempf et al., 1999). Consequently, the facies

relationships were strongly heterochronous across the basin, and terrestrial deposits grade into marine sediments over a lateral distance of few tens of kilometres. This is also the case in the study area, where thick conglomerate packages situated at the Alpine thrust front c. 50 km to the NE of the Aar-massif (Napf conglomerates; Matter, 1964) separate the basin into southeastern and northwestern segments with different lithostratigraphic schemes (Fig. 3a). For simplicity purposes, these areas will be referred to as the eastern and western segments. East of the Napf conglomerates, in the following text denoted as the Napf-units of the OSM (Matter, 1964), the OMM has been grouped in two transgressive-regressive packages referred to as the Lucerne- and the St. Gallen-Formations (Keller, 1989). Both units are separated by a m-thick palaeo-sol (Schlunegger et al., 2016). We will refer to these units as the OMM-I (Lucerne-Fm) and the OMM-II (St. Gallen-Fm), respectively (Fig. 3a). Keller (1989) additionally categorized the OMM-I east of the Napf-units into a lower wave-dominated unit and an upper unit where tidal processes are recorded, which we refer to as the OMM-Ia and OMM-Ib.

West of the Napf and also at the proximal basin border, the OMM has also been categorized in two units (Fig. 3a) but with a different scheme and different names. These are the Sense-Formation at the base (suite of sandstones with mudstone interbeds) and the Kalchstätten-Formation at the top (alternation of sandstones and mudstones). Further up-section, these marine deposits (Strunck and Matter, 2002) grade into the fluvial conglomerates of the Guggershorn-Formation and thus into the OSM (Strunck and Matter, 2002) (Fig. 3a). Magnetostratigraphic dating showed that the accumulation of the Guggershorn-Formation occurred contemporaneously with marine (OMM) sedimentation at more distal sites. These conglomerates thus represent the deposits of a braided stream that shed its material to the OMM sea, similar to the conglomerates in the Napf. As will be put forward in the discussion of this work, the Molasse deposits on the western side of the Napf can be correlated with the OMM-I and OMM-II units on the eastern side (Fig. 3a).

In the central basin near Fribourg, also on the western side of the Napf, sedimentological investigations of sandwaves (Homewood et al. 1980; Homewood and Allen, 1981) disclosed the occurrence of tidal bundles and a bi-directional dispersal of sedimentary material. These deposits have been assigned to a subtidal environment (Homewood and Allen, 1981), where material with sources in the Central Alps were re-distributed in the basin by strong tidal currents (Allen et al., 1985; Kuhlemann and Kempf, 2002). Lithostratigraphic correlations suggest that the deposits at Fribourg most likely correspond to the lower Sense-Fm (Python, 1996) and thus to the OMM-Ia (see discussion, and Fig. 3a).

In the distal basin, between the Lake Neuchâtel and the Wohlen areas (Fig. 2a), coarse-grained sandstones with large-scale cross-beds where individual grains are larger than 2 mm have been interpreted as subtidal sandwaves (Allen et al., 1985). These deposits are either calcareous-sandstones with shelly-fragments, referred to as the "Muschelsandstein" (Allen et al., 1985, Fig. 3a). Alternatively, they occur as coarse-grained cross-bedded sandstones with large litho-clasts, also called the "Grobsandstein" (Jost et al., 2016).

Chronostratigraphic framework

Ages for the OMM deposits have been established by multiple authors through palaeontological analyses of mammalian fragments and teeth (Keller, 1989; Schlunegger, 1996; Kempf et al., 1999) and $^{87}Sr/^{86}Sr$ chemo-stratigraphy (Keller, 1989).

The latter yield a numerical age between c. 18.5 and 17 Ma, particularly for the OMM-II on the eastern side of the Napf. Subsequent magneto-polarity chronologies (Schlunegger et al., 1996; Strunck and Matter, 2002) paired with further micro-mammalian discoveries (Kempf et al., 1997; Kempf, 1998; Kälin and Kempf, 2009; Jost et al., 2016) allowed an update of the chronological framework (Fig. 3b) of Keller (1989) through correlations with the Magneto-Polarity-Time-Scale (MPTS) of Cande and Kent (1992, 1995) and the most recent astronomically tuned Neogene time-scale (ATNTS, Lourens et al., 2004). This yielded in the notion that the transgression of the peripheral sea and the deposition of the OMM started at c. 20 Ma and was synchronous, within uncertainties, across the entire Swiss Molasse basin (Strunck and Matter, 2002). However, a temporal correlation of sections across the Napf, i.e. between eastern and western Switzerland (Fig. 3a), and a harmonization of the stratigraphic schemes (Fig. 3b) has not been accomplished yet. This will be accomplished in this paper, and it will build the temporal framework for the discussion of the development of the basin.

3 Methods

3.1 Sedimentological investigations

Location of sections and available database

Following the scope of the paper, we established the facies relationships and sediment transport patterns during the transgressive phase of the OMM and thus mainly focused on the OMM-I. We proceeded through sedimentological investigations of key-sites (Fig. 2a), which expose the related succession in proximal (Entlen section east of the Napf-units; Sense section west of the Napf-units), central (St. Magdalena site, Gurten drill core) and in distal positions (Lake Neuchâtel and Wohlen areas). The lithofacies in the Entlen and Sense sections was investigated in the field at the scale of 1:50. At each outcrop along these sections, data was collected as notes in the field book and, hand drawings on digital photos (available from the senior author upon request). The results are then presented as logs on Figure 4, and in Tables 1 and 2. The St. Magdalena site and the Lake Neuchâtel and Wohlen areas only display outcrops rather than sections. Therefore, the sediments at these locations have been sketched in the field and on digital photos, thereby paying special attention on collecting information about the orientation and thickness of cross-beds. The sedimentary material of the c. 200 m-deep Gurten drill core is not available. However, the sediments were photographed at high resolution at the University of Bern in 1989 (see supplement Fig. S3). We used these photos to extract information on the lithofacies association encountered in the drilling.

Reconstruction of sedimentary architecture

The lithofacies have been identified (e.g. Schaad et al., 1992; Keller, 1989) based on the assemblage of sedimentary characteristics including: grain size, thickness, lateral extent if applicable, sedimentary structures, basal contact, colour and fossil content (Tables 1 to 5). The lithofacies types correspond to individual bedforms (see Tables 1 to 5 for references), which bear information on flow strengths, flow directions, sediment supply and water depths (e.g., Keller, 1989). The combination of these parameters, usually recorded by distinct assemblages of lithofacies types, can be used to identify distinct sedimentary settings. Related concepts of facies analysis have been documented for fluvial deposits (Miall 1978; 1985; 1996; Platt and

Keller, 1992) but are less standardized for shallow marine deposits. Here, we followed Keller (1989) and Schaad et al., (1992), who developed a concept for shallow marine deposits where lithofacies types are grouped to facies assemblages in a hierarchic order, based on which distinct shallow marine settings can be interpreted. We followed these authors and assembled the various lithofacies types into 5 depositional settings, which are from land to sea: Terrestrial, backshore, foreshore, nearshore and offshore. We then mapped the depositional settings at the scale of 1:25'000 at various sites across the Swiss Molasse basin where suitable outcrops were present (see Fig. 2a for visited sites).

Determination of sediment transport directions

Sediment transport directions were determined from orientations of clast imbrications, gutter casts, and dip directions of cross-beds. In addition, the orientation of the coastline can be inferred from sediment transport within the surf-and-swash zone at the wet beach where rolling grains carve mm-thin rills in the beach deposits, which are oriented perpendicular to the coast. These rills are recorded by linear grooves, or parting lineations, on the surface of sandstones (Allen, J., 1982; Hammer, 1984). We thus measured the orientation of these features where visible. We also determined the strike direction of oscillation-ripple marks to infer the orientation of waves and thus of the coastline.

Calculation of palaeo-water depths

We analysed the sediments in the key sections according to their palaeo-water depths. For oscillation-ripple marks, the ripple metrics (spacing between ripple crests and ripple heights) together with the grain size can be used to infer water depths at the time the oscillation-ripples were formed (Diem, 1985; Allen et al., 1985). We thus measured the ripple metrics with a meter stick together with grain sizes in the field and calculated the water depths following Allen (1997). Likewise, minimum water depths can be inferred form heights of cross-beds as examples from modern streams have shown (Bridge and Tye; 2000; Leclair and Bridge, 2001). Please refer to the supplement for the deviation of the related equations. Published information from deep-drillings (Boswil 1; Hünenberg 1; Schlunegger et al., 1997a) and seismo-stratigraphic data (Line 8307; Schlunegger et al., 1997a, Line BEAGBE.N780025; Fig. S2, supplement) completed the available database.

4 Results

Proximal basin border to the east of the Napf: Entlen section (site 13 on Fig. 2a)

The sedimentary suite of the c. 370 m-thick OMM-Ia at Entlen (Fig. 4a and Fig. S4a in supplement) records a large diversity of lithofacies types (Table 1). Parallel-laminated (Sp), fine- to medium-grained sandstone packages are cm- to dm-thick and normally graded. These deposits alternate with dm-thick low-angle cross-bedded units with tangential lower boundaries (Sc, Sct_a) and layers with a massive structure (Sm). Gravel and pebble layers (Sg) and shell fragments (Shf) are visible where sandstone units have erosive bases. Current- (Scr) and oscillation-ripple marks (Sos), locally with branching crests (Sbr), as well as flame-fabrics or sand-volcanoes (Sv) are present only in some places. Fine-grained lithofacies including mm- to cm-thick parallel-laminated to massive mudstone layers (Mp, Mm). Siltstone climbing-ripples (Mcl) are subordinate in the OMM-

Ia suite. Mudstone drapes (Md), a few mm thick, mostly occur on top of current ripple-marks (Scr). In places, root-casts are associated with yellow- to ocherish-mottled colours.

The overlying c. 430 m-thick OMM-Ib (Fig. 4a and Fig. S4a in supplement) comprises fine- to medium-grained sandstone packages with mudstone interbeds (Table 1). Low-angle trough- (Sct_r) or tabular (Sct_a) cross-bedded sandstone beds are several decimeters thick. The Sct_r-sandstones contain current-ripple marks (Scr) at their base, whereas laminae-sets of Sct_a-sandstones are interbedded with current-ripples (Scr) recording opposing sediment transport direction. At one site, dm-thick sandstone beds display a planar base and a wavy top with a wavelength of several meters (Spw; Fig. 4a). Parallel-laminated (Sp) and massive-bedded (Sm) sandstone beds are dm-thick and mainly found at the top of the OMM-Ib unit. Mudstones mostly occur as mudstone drapes (Md) on top of current ripple-marks (Scr). Lenticular- and flaser-interbeds (Mle, Mfl) are dm thick and characterized by current ripple-marks with truncated crests. The OMM-Ib then ends with a m-thick mudstone displaying yellow to reddish mottling, root casts and caliche nodules.

Estimates of palaeo-water depths (see supplement) reveal that the OMM-Ia sedimentary rocks were deposited in shallow conditions <5 m deep (Fig. 4a and Table S2). At the base of the OMM-Ib palaeo-water depths were >15 m and thus deeper than compared to the OMM-Ia unit (see supplement). The OMM-Ib then shallows towards the top.

Measurements of bedform-orientations of the OMM-Ia deposits reveal sediment transport directions between 315° NW and 60° NE, with a dominant NE-directed transport (Fig. 4a). During OMM-Ib times, transport directions were bi-directional, and measurements reveal the full range between 260° W and 70° E (Fig. 4a). Dominant transport directions of the OMM-Ib sediments change towards the N and to the W up-section.

Proximal basin border in the center: Napf-units (site 12 on Fig. 2a)

The Napf-units, which are a terrestrial interval of the OMM and the OSM (Fig. 3; Schlunegger et al., 1996), are c. 1550 m thick and include a succession of conglomerates, sandstones and mudstone interbeds (Matter, 1964), which we categorize into 5 lithofacies types (Table 2, Fig. S4d in supplement). Individual conglomerate beds are up to 10 m thick and display stacks of 2 – 3 m-thick beds with massive (Gm) to cross-bedded (Gc) geometries. The sandstone beds occur as massive-bedded (Sm) and cross-bedded (Sc) units. Interbedded mudstones are horizontally bedded (Mp) and have a yellowish-reddish mottling, caliche nodules and root cast. Palaeo-flow measurements imply a change from a NE-directed transport during USM-times to a NW-directed sediment transport between OMM-I- and OSM times.

Proximal basin border to the west of the Napf: Sense section (site 7 on Fig. 2a)

The OMM at Sense (Fig. 4b and Fig. S4b) starts with a c. 200 m-thick succession of predominantly sandstones with some mudstone interbeds. Medium- to coarse-grained sandstone beds, up to 2 – 3 m thick, are massive-bedded (Sm), parallel-laminated (Sp) and trough cross-bedded (Sct_r) (Table 3). They also occur as m-scale tabular cross-beds (Sct_a) forming several m-thick sigmoidal fore-sets (Sc) with top- and bottom-sets and pebbly lags (Sg). These packages are well exposed along a nearby road-cut (Heitenried, Fig. 2a; 46°49’27” N / 7°18’42” E; Fig. S4c in supplement). Some of these Sct_r-cross-beds contain

current-ripple marks (Scr), which are draped with a muddy layer (Md). Ripple marks also build up tabular sandstone bodies. They are either asymmetric (Scr) or symmetric (Sos) and may display branching crests (Sbr). In places, the sandstone bodies are highly bioturbated (Sf). Mudstone interbeds are 10 – 20 cm thick, massive- (Mm) to parallel-laminated (Mp) and strongly bioturbated (Mf).

The first-occurrence of 5 – 10 m-thick sandstone beds at 200 m stratigraphic level (Fig. 4b) marks a distinct shift in the stratigraphic record where several m-thick cross-bedded sandstone beds dominate the sedimentary succession. At this level, (i) 5 – 10 m-thick normally graded sandstone beds overlie an erosive base and display epsilon cross-beds (Sce); (ii) cross-bedded sandstones (Sct_a) are several meters thick and tens of meters wide, and individual laminae-sets are superimposed by current ripples (Scr) with an opposite flow direction than the cross-beds themselves; nearly all cross-beds (Sc) are superimposed by mudstone drapes (Md); and (iii) medium-grained sandstones display ridge-and-swale bedform geometries (Spw) with a small amplitude of a few dm and a large wavelength of several m. Some of these Spw-facies are occasionally covered with oscillation-ripple marks (Sos). The Sense section ends with an alternation of dm-thick mudstone beds (Mm) and m-thick massive- to cross-bedded conglomerates (Gm, Gc). These conglomerates then evolve towards an amalgamation of several m-thick, massive- and cross-bedded packages, characterizing the uppermost c. 50 m suite of the Sense section (Fig. 4b).

Estimates of palaeo-water depths range between 5 – 10 m (Fig. 4b and supplement Table S3) during deposition of the lowermost 200 meters. Conditions were deepest at the 200 m stratigraphic level, reaching water depths in the range of up to 30 m (see supplement). Measurements of sediment transport directions cover the range between c. 0° N and 90° E (Fig. 4b) at the base of the Sense section, which then changed to an axial, bipolar SW – NE-directed transport and to a W-directed transport towards the end of the section (Fig. 4b).

Basin axis: St. Magdalena site and Gurten drill core (sites 4 and 9 on Fig. 2a)

The sandstones within a cave-system near Fribourg (St. Magdalena; Fig. 2a and Fig. S4c in supplement) are medium- to coarse -grained and display an amalgamation of up to 1 – 3 m-wide, cross-bedded troughs (Sct_r) with current-ripple marks (Scr) at their base. The cross-bedded troughs and the ripple marks are both covered by mudstone drapes (Md). The amplitude of the troughs is in the range of several dm, whereas the cross-sectional widths span several decimetres to meters. The sandstones also occur as massive-bedded units (Sm). They are occasionally interbedded with current-ripple marks (Scr) draped with mudstone layers (Md). Basal contacts are erosive. Measurements of morphometric properties (St. Magdalena; Fig. 2a) allow an estimation of water depth in the range between c. 3 and 5 m (Table S1, supplement). Sediment transport directions measured at the St. Magdalena site reveal a WSW – ESE-dominated sediment transport.

In the nearby c. 260 m-deep Gurten (Fig. 2a) drill core (Fig. S3, supplement), OMM-Ia deposits occur as cross-bedded sandstones (Sc) topped with mudstone drapes (Md). These lithofacies associations (Table 4) are most abundant within the drill core and make up c. 200 m of the log. However, because drill cores offer limited information about the dimensions of the encountered sediments, we were not able to determine if cross-beds can be assigned to tabular-beds (Sct_a) or to troughs (Sct_r).

Distal basin border in the west and the east: Lake Neuchâtel and Wohlen areas (sites 2 and 16 on Fig. 2a)

Calcareous, shelly-sandstones (Scc) occur at distal sites in the western and eastern Molasse basin and are an assemblage of various lithofacies. This Scc-facies association is made up of 5 – 10 m-thick, coarse-grained sandstone beds with low-angle cross-beds (Sc) that contain coquinas and shell-fragments (Shf) and pebbles (Sg) in places. Interbedded fine-grained sandstones contain current-ripple marks (Scr) recording an opposite flow direction relative to the cross-beds (Sc).

In the west (sites at Lake Neuchâtel area; Fig. 2a and Fig. S4c in supplement), mapping shows that Scc-"Muschelsandstein" deposits are c. 5 m thick and record NNE- to NE-directed sediment transport. Foreset thicknesses of these deposits thin to <1 m towards the front of the Napf-megafan, where herringbone cross-beds imply SW and NE-directed, bi-modal sediment transport. At the NE margin of the Napf, these Scc-"Muschelsandstein" deposits grade into Slc-"Grobsandstein" units, which show m-thick tabular cross-beds (Sct_a) or dm-thick trough cross-beds (Sct_r) where individual troughs have m-wide diameters. Measurements of palaeo-flow directions reveal a SW- and SE-directed transport. These deposits are either time-equivalent sediments of the Scc-"Muschelsandstein" and thus contemporaneous with the OMM-Ib succession, or they mark the base of the OMM-II succession (Jost et al., 2016). Farther east near the Wohlen area (Fig. 2a and Fig. S4d in supplement), foresets of "Muschelsandstein" cross-beds are 6 to 8 m thick, and in some locations up to 10 m thick as reported by Allen et al. (1985). Sediment transport directions were oriented towards the SSW covering the range between 230° SSW and 250° WSW and striking parallel to the topographic axis. Estimates of water-depths of the Scc-"Muschelsandstein" reveal palaeo-water depths (Table S1, supplement) between 60 and 100 m.

5 Sedimentological interpretation

Entlen section

The OMM-Ia sedimentary rocks of the Entlen section are assigned to a backshore to upper nearshore realm, within a wave-dominated environment (Fig. 4a, and please see Table 1 for references). Records of waves are inferred from: (i) tabular, parallel-laminated and normally graded (Sp) sandstones, which are interpreted to represent sediments of the surf-and-swash zone near the wet beach where sedimentation occurs in the upper flow regime; (ii) low-angle cross-beds (Sc) with pebbly lags and shell fragments (Shf), which could reflect sand-reefs (or shoals), rip channel fills or storm layers, and (iii) oscillation- (Sos) as well as branching-ripple marks (Sbr) pointing to wave-activity (Fig. 4a). Gravels and pebbly-lags (Sg) are either evidence for high-energy storm events or for river inflow from the backshore. Finer-grained lithofacies, which are either indicative of rapid sedimentation (Sv, Mcl, Table 1) or incipient pedogenesis (Mp, Mm; Table 1), are consistent with a shallow marine, wave-dominated environment.

The basal part of the OMM-Ib suite is assigned to a foreshore to lower nearshore setting, shaped by the combined effect of wave- and tidal-activity (Fig. 4a). This is inferred by the observation that current ripple-marks (Scr), which are situated on top of lamina sets of tabular- (Sct_a) and trough-cross-beds (Sct_r), point towards an opposite flow direction than the cross-beds themselves (Fig. 4a). Mudstone drapes (Md) on top of ripple marks together with lenticular- and flaser-interbeds (Mle, Mfl),

are supportive evidence for a tidal environment (references in Table 1). The occurrence of waves, however, is inferred from parallel-laminated sandstones (Sp) with parting lineations, and ridge-and-swale (Spw) structures at the base of the OMM-Ib-suite. Towards the top of the OMM-Ib, massive sandstones (Sm) and mudstones with mottled colours, root casts and caliche nodules mark the presence of a backshore, possibly terrestrial setting.

The change from a nearshore, wave-dominated environment (OMM-Ia) to an environment with tidal records (OMM-Ib) was additionally associated with a deepening from <5 m to >15 m, particularly at the base of the OMM-Ib. We thus consider the base of this unit as the maximum-flooding surface (MFS), separating the OMM-I into a transgressive OMM-Ia unit and into a regressive OMM-Ib succession (Figs. 4a and 5a).

Napf-units

We interpret the association of massive (Gm) to cross-bedded (Gc) conglomerates, and massive- to cross-bedded sandstones (Sm, Sc) as deposits within a braided river system (Table 2, see references there). In such an environment, conglomerates are common records of active channels. Massive- (Sm) to cross-bedded (Sc) sandstones alternating with mottled mudstones were most likely formed on the floodplains bordering the network of braided channels, when bursts resulted in the accumulation of crevasse-splay deposits (Platt and Keller, 1992). Mudstone interbeds (Mp) with evidence for palaeo-sol genesis formed when channel belts shifted away from the axis of the section (Platt and Keller, 1992). This facies-association was mapped over tens of kilometres, both across and along strike of the basin orientation. It is thus assigned to an alluvial megafan (Schlunegger and Kissling, 2015).

Sense section

We assign the OMM of the Sense section to a tidal-dominated environment where deltaic estuaries dominated the sedimentary facies (Fig. 4b and please see Table 3 for references). This is inferred from: (i) sigmoidal cross-bedded sandstones (Sc) with distinct top-, fore- and bottom-sets and pebbly-lags (Sg) that are indicative of a delta, and (ii) trough cross-bedded (Sct_r) and massive bedded (Sm) sandstones that could represent mouth-bar deposits where estuaries (or tidal intlets) end. In such an environment, current-ripple marks (Scr) with mudstone drapes (Md) at the base of tabular cross-beds (Sct_a) point to rhythmic changes of tidal-current slack water stages within a subtidal setting, whereas ripple-marks (Sos) with branching crests (Sbr) and parallel-laminated sandstones (Sp) were most likely formed under the influence of waves close to the beach. Massive-bedded (Mm), parallel-laminated (Mp) and strongly bioturbated (Mf) mudstone interbeds are assigned to a tidal flat that established on the landside margin of the delta. Towards the top of the section, the facies successively evolves into a fan delta setting. This is inferred from the observation that the conglomerate beds become more frequent and more continuous and display several m-thick beds, with massive- to cross-bedded geometries (Gm, Gc).

The first-occurrence of 5 – 10 m-thick sandstone beds at 200 m stratigraphic level (Fig. 4b) records a remarkable increase of the water depth, when 5 – 10 m-deep tidal channels (Sce-sandstone beds with epsilon cross-beds) grade into several m-thick subtidal sandwaves (Sct_a) and nearshore tempestites (m-scale Spw-sandstones with ridge-and-swale geometries, see Table 3

for lithofacies and references). These two latter lithofacies (Sct_a, Spw) are interpreted to record the deepest palaeo-water depth in the Sense section, when water depths were in the range of up to 30 m. We consider this stratigraphic level to record the maximum-flooding surface (MFS) within the Sense section (Fig. 4b), and we will use it for correlation purposes with the OMM succession at Entlen (see discussion).

St. Magdalena site and Gurten drill core

The several m-thick outcrops near Fribourg are interpreted as subtidal shoal deposits, which accumulated within a tide-dominated environment (Table 4, see references there). This is inferred from: (i) m-scale cross-bedded troughs (Sct_r) with current-ripple marks (Scr) at their base (see also Homewood et al., 1981; for a similar interpretation). Alternatively, sandstone troughs (Sct_r) could be assigned to a mouth-bar environment, where massive-bedded sandstones (Sm) would represent records of rapid sedimentation. In contrast, mudstone drapes (Md) on top of the ripple-marks (Scr) and cross-beds (Sc) are formed during low-energy tides, or possibly during slack stages. Similar deposits (Sct_r, or possibly Sct_a) within the Gurten drill core could also be interpreted as sediments of subtidal shoals, however, due to limited exposure, interpretations are non-conclusive. Shallow palaeo-water depths are also inferred from estimates of water depths ranging between 3 and 5 m.

Lake Neuchâtel and Wohlen areas

We interpret the Scc-"Muschelsandstein" (Table 5) sediments (containing coquinas and shell-fragments (Shf) and pebbles (Sg)) to have been deposited within the topographic axis of the Burdigalian seaway, (see also Allen et al., 1985, and Jost et al., 2016, for a similar interpretation). Meter-scale cross-beds (Sct_a), locally superimposed by current-ripple marks (Scr), have been interpreted to reveal deposition under strong tidal currents (Allen et al., 1985). These deposits are thus assigned to offshore, tide-dominated sandwaves, where sediment transport was NNE- (Lake Neuchâtel area; Fig. 2a) or SSW-directed (Wohlen area, Fig. 2a). In places, pebbly-lags (Sg) are interpreted as flood-related splays of gravels into the offshore setting, derived from the neighbouring Napf-megafan. In contrast, the coarse-grained sandstones (Slc-"Grobsandstein" sediments; Table 5) reveal similarities to the subtidal-shoal deposits encountered at the St. Magdalena site where trough cross-bedded sandstones (Sct_r) and tabular cross-beds (Sct_a) dominate the facies assemblages. However, the deposits in the Wohlen area are coarser-grained, and cross-beds (Sc) have larger diameters, but similar thicknesses. We relate the coarse-grained nature of these deposits to the proximity of the Napf-megafan in the SW. The cross-beds with larger wavelengths and similar amplitudes possibly imply stronger currents compared to the subtidal shoal-deposits near St. Magdalena.

6 Discussion

6.1 Re-appraisal of chronostratigraphic framework

Entlen section

No magnetostratigraphic data is available for the Entlen section, but a temporal calibration of the deposits can be achieved through indirect lines of evidence. This particularly concerns the reconstruction of an age constraint for the basal transgression,

which is accomplished using two lines of evidence: First, the transgression post-dates the deposition of the USM, which terminated at C6An1 at the Fischenbach-section (Fig. 3b; Schlunegger et al., 1996). Second, based on stratigraphic interpretations of palaeo-flow direction data Strunck and Matter (2002) considered that the transgression of the OMM progressed from the east towards the west, where the first marine sediments have been dated with C6r in the Sense section (Figs. 3b, see next section). An E – W transgression of the OMM is also seen in seismic line BEAGBE.N780025 (supplement, Fig. S2), where OMM deposits onlap onto the USM in a westward direction. Accordingly, the onset of the OMM at Entlen on the eastern side of the Napf predates the transgression at Sense farther west. Based on these arguments, we set an age of c. 20 Ma for the base of the OMM-I in the eastern Swiss Molasse basin (Figs. 3b and 5), which is consistent with Kälin and Kempf (2009). For the top of the OMM-I, we determine an age using the magneto-stratigraphy of the Napf-section (Fig. 3b) c. 10 km to the west of Entlen. This section includes an alternation of 6 reversed- and 5 normal-polarized magnetozones (Schlunegger et al., 1996). The lowermost, very long normally polarized interval (N1, Fig. 3b) includes the mammalian fossil site Hasenbach 1 recording an MN3b age (Schlunegger et al., 1996) or even a lower-MN3b age, as a revision of the mammalian material has shown (Kälin and Kempf, 2009). This allows a correlation of the normally polarized interval N1 with chron 5En of the MPTS (Cande and Kent, 1992, 1995) or the ATNTS (Lourens et al., 2004), respectively (Fig. 3b). Since the third reversed magnetozone of the Napf-section is very short (R2), and since the ATNTS chron 5D spans several 100 kyr and is thus quite long, it is most likely that a hiatus encloses C5Dr2 to C5Dr1 (Fig. 3b). In addition, because (i) the change from MN3b to MN4a has been calibrated with C5Dr2 (Jost et al., 2016), and since (ii) the base of the overlying OMM-II (Figs. 3b and 5) has been dated with MN4 (Keller, 1989), we suggest that the inferred hiatus coincides with the boundary between the OMM-I and the OMM-II (Figs. 3b and 5). This age assignment is consistent with magneto-polarity stratigraphy in the Molasse basin c. 70 km farther east (Kempf and Matter, 1999). It is also consistent with micro-mammalian investigations in the distal Molasse basin c. 30 farther north where Jost et al., (2016) found that deposits spanning MN3b and MN4a are missing. Based on these constraints, we suggest that the top of the OMM-I correlates with C5Dr of the MPTS or C5Dr2 of the ATNTS, respectively, followed by a c. 0.5 Ma-long hiatus (Figs. 3b and 5). According to this correlation, the sediments recording the maximum-flooding conditions in the Entlen section are c. 19 Ma old.

Wohlen area

Correlations of the OMM deposits from the Entlen section to the Wohlen area was accomplished by Schlunegger et al., (1997a) through a seismostratigraphic analysis of the seismic line 8307 (Fig. 2a). The seismic data shows that the OMM-I deposits onlap onto USM strata and then overlap this unit (Fig. 5b). Schlunegger et al. (1997a) correlated the OMM-I sequence with their Unit B in the Entlen section, which corresponds to the top of the OMM-Ia in our stratigraphic scheme. In addition, our field investigations and micro-mammalian data by Jost et al. (2016) revealed that the “Muschelsandstein” follows on top of the OMM-Ia and most likely corresponds in age to the OMM-Ib. Based on these arguments, we constrain the deposition in the distal basin to the time interval between c. 19 and 18 Ma (Fig. 5b). However, based on seismostratigraphic investigations of line 8307, Schlunegger et al. (1997a) proposed that sedimentation was interrupted at c. 18 Ma by a c. 0.5 Ma-long or possibly

longer hiatus. This time span has later been specified through new micro-mammalian discoveries by Jost et al. (2016), who noted that a record of MN4a is missing in the Wohlen area and that the base of the OMM-II hosts mammalian fragments that correspond to MN4b. The interpretation of an inferred unconformity is additionally supported through observations of vadose cements (Allen et al., 1985) within the "Muschelsandstein", and through evidence for a thick palaeo-sol separating OMM-I from OMM-II in the Entlen section (see chapter 4 and 5). We use the occurrence of vadose cements and the palaeo-sol to propose that the uppermost beds of the OMM-Ib (including the "Muschelsandstein") were exposed to erosion, or non-sedimentation, after deposition. Furthermore, because the "Muschelsandstein" unit records the deepest water depth during OMM times at distal sites, we tentatively suggest that deposition of these mega-sandwaves started at the same time when the deepest conditions (MFS) were recorded within the Entlen section (Fig. 5b).

Sense section

Magnetostratigraphic data for the Sense section was presented by Strunck and Matter (2002). These authors placed the USM/OMM-boundary at this site within C6r of the MPTS (Cande and Kent, 1992; 1995), or alternatively of the ATNTS (Fig. 3b; Lourens et al., 2004). The subsequent alternation of normal and reverse magnetozones was correlated by these authors with chrons 6r through 5Dn of Cande and Kent's MPTS (1992; 1995), the latter of which corresponds to C5Dn1 of the ATNTS (Lourens et al., 2004). Following Strunck and Matter (2002), a possible hiatus prior to c. 17.5 Ma is likely to be recorded also within the Sense section (Figs. 3b and 5a). This correlation implies that the lower Sense-Formation corresponds to the OMM-Ia, whereas the upper Sense-Fm and the Kalchsätten-Fm are time equivalent units of the OMM-Ib (Figs. 3a, 3b). The topmost 50 m of the Kalchstätten-Fm, where the base was characterized by the first appearance of conglomerates, follows upon this hiatus and corresponds to the OMM-II in our scheme (Figs. 3 and 5a). This further implies that a hiatus separates OMM-I from OMM-II across the entire basin (Fig. 5a). In addition, subsequent sedimentation (base of OMM-II) progressed from the west to the east (Fig. 5a). In the same sense, the sediment packages recording the maximum-flooding conditions (MFS) have most likely the same age across the entire basin (Fig. 5a).

Lake Neuchâtel area

No micro-mammalian sites have been reported for the OMM deposits in the distal western Molasse basin. Therefore, we cannot provide further constraints on the history of sedimentation. However, our field inspections in the area of Lake Neuchâtel (Fig. 2a) show a sedimentary succession similar to that in the east, where amalgamated sandstone beds are overlain by the "Muschelsandstein" unit. Our field inspections also show that these calcareous, shelly-sandstones thin from c. 10 m in the Lake Neuchâtel area in the west to a few meters towards the distal margin of the Napf-megafan, consistent with the results by Allen et al. (1985). Because of the architectural similarity between the "Muschelsandstein" deposits in the east and the west, we tentatively consider that deposition of the "Muschelsandstein" occurred synchronously across the entire Swiss Molasse basin.

6.2 Evolution of the Molasse basin

The chronostratigraphic framework together with the sedimentological data and palaeo-flow directions are used to propose a scenario of how the basin evolved through time. During USM-times (Fig. 6a), prior to the Burdigalian transgression, the basin was occupied by alluvial megafans at the proximal basin border, which gave way to an axially-directed channel-belt system in the distal basin (Fig. 6a; Kuhlemann and Kempf; 2002). Analysis of heavy-mineral assemblages by Füchtbauer (1964) and measurements of palaeo-flow directions in our study area (sole casts, and cross-beds, this paper) and in eastern Switzerland (Kempf et al., 1999) revealed a NE-directed material transport towards the Munich region (Fig. 6a). In this area, the Molasse streams ended in a peripheral sea where neritic- to open-marine conditions prevailed (Kuhlemann and Kempf, 2002). Within the basin, a possible divide for sediment transport was situated somewhere SW of Geneva. We infer such a separation of sediment dispersal because orientation of tidal cross-beds to the South of Geneva (Allen et al., 1991; Allen and Baas, 1993) imply a sediment dispersal towards the Tethys, whereas our own and published data from the Swiss part of the Molasse basin reveal a northeast-directed transport to the Paratethys in the NE.

The palaeo-geographic situation at c. 20 – 19 Ma is shown in Fig. 6b. It illustrates that the central part of the Molasse basin changed to a shallow-marine sea, which was c. 40 km wide at that time. Our estimates of palaeo-bathymetic conditions and sedimentological data (Figs. 4a and 4b) reveal that the water depths corresponded to a subtidal and nearshore setting. Nearshore to possibly offshore conditions (30 – 50 m) are recorded by subtidal mega-sandwaves (Allen and Bass, 1993) south of Geneva and by the predominance of sandstone-mudstone-alternations within the Boswil and Hünenberg drill cores in the NE (Wohlen area, Fig. 2a; Schlunegger et al., 1997a). Subtidal shoals, in up to 5 m-deep water, occupied the western part of the central Swiss Molasse (Fig. 6b). This was already proposed by Homewood and Allen (1981), and it is here confirmed by our sedimentological data and estimates of palaeo-water depths (supplement). Measurements of sediment transport directions from the shoal deposits reveal bi-modal, SW-NE-directed transport, with a dominant NE-orientation. This is particularly the case at the proximal basin border near the Sense section (Fig. 2a) where deltaic foresets accumulated within an estuarine-setting (Fig. 4b). Mapping of depositional settings allowed us to trace the shoal deposits towards the northern tip of the Napf-megafan, from where the shoals narrow from c. 20 km to c. 10 km over a 70 km-long distance along strike. It thus appears that the shoals were deflected towards the topographic axis through a dominant NE-directed material transport (Fig. 6b). This interpretation is additionally supported by measurements of the transport directions of the Napf-megafan (i.e. clast imbrications) and the coastal deposits at the Entlen section (i.e. parting-lineation, cross-beds) pointing a material transport towards the NE (Figs. 4a and 5a). At the distal margin of the basin, field inspections show that beach sandstones gave way to subtidal-shoal deposits up-section. South of Geneva, sediment transport was oriented to the SW. This is indicated by the orientations of cross-beds (Allen and Bass, 1993; Fig. 6b). It thus appears that the central Swiss Molasse was a region of sediment export to the northeast and to the southwest. Material transport was most likely accomplished through strong tidal currents (Bieg et al., 2008).

The situation during c. 19 – 18 Ma (Fig. 6c) started with the time when the maximum-flooding surface was formed in the depositional record (MFS; Figs. 5a and 5b). The sedimentological data reveals that this time was characterized by a widening of the basin to widths up to 80 km, and it was dominated by offshore conditions in the topographic axis with water depths >50

m, as the "Muschelsandstein" deposits imply (Fig. 6c). There, cross-bed orientations (our measurements and data by Allen et al., 1985) and heavy mineral assemblages (Allen et al., 1985) reveal that sediment transport in the distal east (Wohlen area) occurred towards the SW, whereas sediment dispersal in the distal west (Lake Neuchâtel area) was directed towards the NE. We use this information to propose that a sedimentary depocenter established at the northern tip of the Napf-megafan. In addition, this megafan is interpreted to have experienced a backstepping. We infer such a scenario from the first appearance of a bi-modal E-W-orientation of material transport in the Entlen section (Fig. 5a). Because an E-W-oriented sediment transport requires a free-passage for tidal currents along the southern basin margin, the sea-side margin of the Napf megafan had to step back to allow such a passage to form (Figs. 6b and 6c).

The palaeo-geographic situation shown in Fig. 6d comprises the timespan between c. 18 and c. 14 Ma and displays the evolution from the OMM-II to the OSM. The OMM-II period followed a period of erosion and non-sedimentation across the entire Swiss Molasse basin, as our re-assessment of the chronological framework of the OMM reveals (Figs. 5a and 5b). This is additionally supported by data from the seismic line in the Wohlen area (Schlunegger et al., 1997a), and vadose cements found in the "Muschelsandstein" (Allen et al., 1985). In addition, measurements of sediment transport directions reveal a SW-oriented sediment transport at proximal positions (Fig. 5a). This also implies that a possible E-W divide for sediment transport shifted towards the region near Munich, or even farther east. We infer such a scenario from the supply of material with sources in the Hercynian basement north of Munich (Fig. 1a) or the Bohemian-massif ("Graupensandrinne", Fig. 6d; Allen et al., 1985; Berger, 1996; Berger et al., 2005; see also setting), which implies a westward tilt of the basin axis. This period ended with the progradation of the alluvial megafans during the time of the OSM.

In conclusion, the establishment of the Burdigalian seaway was accompanied by: (i) a deepening and widening of the basin, including a northward shift of the topographic axis to the distal basin margin, where offshore and thus deepest marine conditions established at 19 Ma, (ii) a reversal of the sediment transport direction from an originally NE-oriented sediment dispersal during OMM-I times, to a SW-oriented sediment transport during deposition of the OMM-II, and (iii) the establishment of a wave-dominated coastline (with some tidal records) on the eastern side of the Napf (Fig. 4a), whereas a tide-dominated estuarine environment characterized the proximal coastal margin on the western side of the Napf (Fig. 4b).

6.3 Controls on the transgression of the OMM

Possible controls on the reversal of the drainage direction and the widening of the basin

We relate the reversal of the drainage direction between the OMM-I and the OMM-II at c. 18 Ma to tectonic processes operating at deeper crustal levels beneath the Alps. This interpretation is guided by a publication of Pfiffner et al. (2002), who related changes in sediment dispersal within the basin to a possible tilt of the foreland plate, caused by the westward shift of the Ivrea body. This tectonic unit comprises mantle rocks with a high density (Fig. 1a) and could thus have influenced the deflection of the foreland plate (Pfiffner et al., 2002). We present a possible geodynamic scenario to explain the 18 Ma-old change in the drainage direction in the next section, but we also acknowledge that this interpretation is speculative at this stage

and warrants further investigations. Such an exploration, however, requires that the geodynamic processes prior to 20 Ma are also considered.

Between 33 and 30 Ma, beneath the Central Alps of Switzerland, the continental lithosphere of the European plate started to enter the subduction channel underneath the Adriatic continental plate (Schmid et al., 1996), while subduction of the European oceanic lithosphere continued beneath the eastern Alps, as palinspastic restorations revealed (Handy et al., 2015). Beneath the Swiss Alps, incipient subduction of the buoyant continental material was considered to have triggered the break-off of the subducted oceanic lithosphere (Schmid et al., 1996). The consequence was the rise of the Alpine topography and a large sediment flux to the Swiss Molasse basin (Sinclair, 1997; Kuhlemann et al., 2001a; 2001b; Willett, 2010; Garefalakis and Schlunegger, 2018), which became overfilled at c. 30 Ma (Sinclar and Allen, 1992; Sinclair, 1997; see also 2.1). East of Munich, however, the basin still remained underfilled until c. 20 Ma as evidenced by deep marine sedimentation, where debris flows and proximal turbidites accumulated within the basin axis (Fertig et al., 1991; Malzer et al., 1993). We use these observations to propose that vertically-directed slab-load forces were still downwarping the foreland plate beneath the eastern Eastern Alps to allow such a deep trough to form, while slab break-off beneath the Central Alps caused a rebound of the foreland plate in Switzerland (Schmid et al., 1996; Schlunegger and Castelltort, 2016). This most likely resulted in a stronger deflection of the European foreland plate beneath the Eastern Alps compared to the Central Alps, which could explain east-directed sediment transport prior to c. 20 Ma (Fig. 6a).

Between c. 20 – 17 Ma, i.e. during OMM-times, a remarkable change was recorded in the Molasse basin. The eastern Molasse basin experienced a change from deep to shallow marine conditions (Kuhlemann and Kempf, 2002), while the Swiss Molasse basin recorded a reversal of the drainage direction from the E to the W, and sediment with an eastern provenance signal was supplied to the Swiss Molasse basin through the “Graupensandrinne” (Kuhlemann and Kempf, 2002; see also 2.1). We relate this reversal in the dispersal of sedimentary material to a SW-directed tilt of the foreland plate, possibly caused by a change in the pattern of slab-load forces underneath the Alps. Particularly, in the eastern Molasse basin, the change from deep to shallow marine conditions could reflect slab unloading through delamination, or break-off, of the subducted European lithosphere (Ustaszewki et al., 2008), while roll-back subduction of the European plate beneath the Central Alps of Switzerland continued, as Kissling and Schlunegger (2018) proposed. The causes for the along-strike differences in the subduction mechanisms are not clear at this stage and could either be related to (i) inheritance related to the Mesozoic phase of rifting (Schmid et al., 2004; Handy et al., 2010), (ii) differences in the mechanical strengths of the foreland plate between the Swiss and the German/Austrian Molasse basins (Tesauro et al., 2009; 2013), (iii) and possible differences in rheological conditions as discussed by Mey et al. (2016). In addition, also at 20 Ma, we propose that the velocity of roll-back subduction beneath the Central Alps of Switzerland was likely to have accelerated. We justify this interpretation through the observation that (i) tectonic exhumation of the Lepontine dome (Fig. 1), accomplished through slip along the Simplon detachment fault (Mancktelow and Grasemann, 1997) occurred at the highest rates at that time (Boston et al., 2017; Schlunegger and Willet, 1999), and that (ii) the rapid rise of the Aar-massif (Fig. 1) also commenced at 20 Ma (Herwegh et al., 2017). Following Kissling and Schlunegger (2018), these processes require a mechanism where several tens of km-thick buoyant crustal material

was delaminated from the subducting European continental plate and accumulated within the crustal root (Fig. 7) within a short time period. Such a rapid phase of roll-back subduction would also shift the basin axis to more distal sites, as proposed by Kissling and Schlunegger, (2018; see their Fig. 7). We use these mechanisms to explain the cross-sectional widening of the Molasse Basin at 19 Ma and the northward shift of the basin axis (Fig. 7), thereby giving way to the deposition of the offshore "Muschelsandstein" (Figs. 6b and 6c). This lithofacies association has been mapped along the distal basin border adjacent to the external massifs only.

Controls on the establishment of a wave-dominated coast in the east and tidal records in the west

Roll-back subduction and the related delamination of crustal material from the subducting European foreland plate was also considered to have resulted in the rise of the Aar-massif (Herwegh et al., 2017), which in turn was likely to have increased the topography surrounding this massif, thereby forming a positive anomaly in the topographic load in the region (Fig. 7). We elaborate the details of these relationships in the following section and then relate the along-strike differences in the depositional environments (wave-dominated coast to the east of the Napf, and estuaries on the western side) to these processes. Structural mapping in the Aar-massif (Wehrens, 2015; Wehrens et al., 2017) has revealed that crustal blocks were rising along steeply SE-dipping thrust faults (Fig. 1b). Accordingly, roll-back subduction, the related delamination of crustal material and the rise of the Aar-massif (Herwegh et al., 2017; Fig. 1b) also lifted the topography above the Aar-massif to higher elevations (Fig. 7). We base this interpretation on the re-routing of the drainage systems (Kühni and Pfiffner, 2001) around the region of this external massif, which possibly commenced at that time. As a result, the topographic loads on the foreland plate were likely to have increased in this area. Sinclair et al. (1991) and Sinclair (1996) explored a possible stratigraphic response to topographic loading, associated with uplift of the Aar-massif (Sinclair et al., 1991), through the application of a linear elastic plate model where thrusting and erosion are dynamically coupled. In their model, the distance between the location of thrusting (Aar-massif) and the site in the basin where a signal is expected depends primarily on the flexural rigidity (or alternatively the elastic thickness or the *Te*-value) of the crustal rocks underlying the foreland basin (Sinclair, 1996). The flexural rigidity of the rocks beneath the Swiss Molasse basin has been quantified with an elastic thickness of c. 10 km using stratigraphic constraints (Sinclair et al., 1991). This estimate is particularly based on thickness gradients of accumulated Molasse deposits across a section from the distal basin border to the Alpine thrust front. This pattern, however, could have been influenced by upper crustal in-homogeneities (Waschbush and Royden, 1992) such as e.g. pre-existing faults (Pfiffner, 1986). This could explain why estimates of *Te*-values that are based on stratigraphic data are lower (Sinclair et al., 1991; Schlunegger et al., 1997b) than estimates that are based on the curvature of the entire European foreland plate from the distal Molasse border to the core of the Alps and even deeper (Pfiffner et al., 2002; Schlunegger and Kissling, 2015). If we consider a local, and thus upper crustal response to loading, characterized by a *Te*-value of c. 10 km (Sinclair et al., 1991; Schlunegger et al., 1997b), then shifts in surface loads through the km-thick stacking of additional material in the Aar-massif is likely to have resulted in the formation of several tens of meters of supplementary accommodation space at the proximal basin border, as the models of Sinclair et al. (1991) predict. As a result, depocenters in the Molasse basin are predicted to step back to proximal positions

(Sinclair et al., 1991), which is consistent with our interpretation of the flow directions and the related implications for the deposition of the Napf conglomerates (see chapter 6.1, and Fig. 6). In addition, according to Sinclair (1996), upward-directed bulging of a few tens of meters is expected at the distal (forebulge) and at the lateral margins of the load (lateral bulge). The spacing between an expected lateral bulge and the location of the surface forcing ranges between 50 – 100 km (using a *Te*-value of 10 km), which is consistent with the distance between the Aar-massif and the inferred subtidal-shoals in the western Swiss Molasse basin (near Fribourg; Figs. 2a and 6b). Because the plate had an eastward tilt at that time, as inferred from palaeo-flow directions, such a flexural signal could possibly not be recorded on the eastern side of the Aar-massif where the marine conditions were too deep (Figs. 6b and 6c). We additionally use these mechanisms to explain the development of different depositional environments at the proximal basin border of the Swiss Molasse Basin. East of the Napf-megafan, a relatively high subsidence (rate of c. 340 m/Ma for OMM-Ia and c. 430 m/Ma for OMM-Ib, based on data in Fig. 4a) most likely resulted in a steeper submarine gradient compared to the west, where the inferred bulging possibly lowered and subdued the submarine slopes (subsidence rate of c. 285 m/Ma for both OMM-Ia and OMM-Ib, based on data in Fig. 4b). This could explain why the evidence for wave action is predominantly recorded along the eastern proximal steeper basin margin. Indeed, investigations on modern coasts have shown that steeper coasts tend to promote the formation of larger waves (Flemming, 2011). In contrast, in the western Swiss Molasse, estuaries and tidal-channels could develop as the wave energy decreased in the subdued coastal landscape. Note, we cannot fully exclude that uplift along basement faults beneath the Molasse basin in western Switzerland (Spicher, 1980) shifted the peripheral sea to shallower bathymetries during OMM-times. If such a mechanism did occur, then it could have amplified the effects related to flexural bulging (Waschbusch and Royden, 1992).

Controls related to changes in sediment supply

The time around 20 Ma was also characterized by a continuous reduction in sediment flux from originally 25'000 km^3/Ma prior to c. 20 Ma to c. 15'000 km^3/Ma thereafter (Kuhlemann, 2000; Kuhlemann et al., 2001a, 2001b), which could have contributed, together with the tectonic widening of the basin, to the transgression of the peripheral sea in Switzerland (Fig. 8). The mechanisms leading to this reduction in surface mass flux are not fully understood (Kuhlemann et al., 2002), and multiple hypotheses have been proposed including: (i) shifts towards a dryer palaeo-climate paired with a widespread exhumation of crystalline rocks with low bedrock erodibilities (Schlunegger et al., 2001); (ii) tectonic exhumation of the Lepontine through slip along the Simplon detachment fault, which occurred in response to rapid roll-back subduction (see above and Kissling and Schlungger, 2018). Tectonic exhumation was considered to have shifted the drainage divide farther to the north, thereby substantially decreasing the source area of the Molasse basin (Kuhlemann et al., 2001a); and (iii) uplift of the Aar-massif, which was considered to have resulted in a reorganization of the Alpine streams and which was also associated with a reduction of the source area of the Molasse basin (Kühni and Pfiffner, 2001). Except for the palaeo-climate hypothesis, all other mechanisms are ultimately linked to the tectonic processes we have outlined in the sections above.

Controls related to changes in eustatic sea levels

Whereas tectonic processes are recorded in the arrangement of depositional systems in the entire Swiss Molasse basin, signals related to the eustatic changes of sea level are possibly recorded by several hiatuses. This particularly concerns the times of non-sedimentation between OMM-I and OMM-II, and between the OMM- and the OSM-phase, which we have elaborated in chapter 5.1 (Figs. 5a and 8). In this context, $\delta^{18}O$-values measured on benthic foraminifera have been used as proxy for establishing patterns of sea level changes (Miller et al., 1998). In particular, a shift to more positive values of the stable oxygen isotope $\delta^{18}O$ implies a growth of polar ice sheets, where lighter oxygen isotopes ($\delta^{16}O$) are preferentially stored (Zachos, 2001). As a consequence, global sea level most likely decreased (amplitude of drop is not really known) during shifts towards heavier (and thus more positive) isotopic records in planktonic organisms (Miller et al., 1998). These patterns have been reconstructed by Miller et al. (1996; 1998) at a high resolution. Shifts towards larger $\delta^{18}O$-values generally coincide with times when hiatuses are recorded in the Molasse basin (Fig. 8; see also Pippèrr and Reichenbacher, 2017; Sant et al., 2017). We thus suggest that drops in global sea level of a few tens of meters initiated a phase of no deposition in the Swiss part of the Molasse basin, at least between OMM-I and OMM-II at c. 18 Ma, and between the OMM and the OSM.

7 Summary and Conclusion

In summary, we suggest that the Burdigalian transgression was related to a combination of a deepening and widening of the basin and a reduction of sediment supply rates, which we ultimately relate to tectonic processes in the Alpine hinterland. In this context, we consider that roll-back subduction was most likely responsible for the widening of the basin in the foreland and for the shift of the basin axis to distal positions. In addition, roll-back subduction of the European mantle lithosphere and delamination of crustal material most likely resulted in the rapid exhumation of the Lepontine dome (Boston et al., 2017) and the associated rise of the Aar-massif (Herwegh et al., 2017). In the Alpine hinterland, these processes occurred simultaneously with a slip along the Simplon detachment fault and thus with a change in the configuration the drainage network (Schlunegger et al., 2001; Kühni and Pfiffner, 2001), with the consequence that the sediment flux to the basin decreased. This reduction in sediment flux, together with the tectonic widening of the basin, was thus likely to have controlled the transgression of the peripheral sea in Switzerland (Fig. 8). In addition, shifts in surface loads, caused by the rise of the Aar-massif, resulted in flexural adjustments in the Molasse basin. This could explain the development of distinct depositional environments and the formation of subtidal-shoals where a lateral bulge is expected. Because of the formation of shallow marine conditions, subtle changes in eustatic sea level contributed to the occurrence of several hiatuses (Sant et al., 2017). Whereas these mechanisms are capable of explaining the establishment of the Burdigalian seaway and formation of distinct sedimentological niches in Switzerland, the drainage reversal during OMM times possibly requires a change in the tectonic processes at a scale that includes the subduction history of the entire mountain range, at least between the Eastern and Central Alps. Current explanations are still speculative and await the results on ongoing research in the framework of the AlpArray initiative. At this stage, we conclude that the geodynamic processes in the Alps including: subduction mechanisms, delamination of crustal material and uplift of the Aar-massif, reorganization of the drainage network and lower sediment flux are reflected in the Swiss

Molasse basin through the establishment of shallow marine conditions and a shift of the topographic axis towards more distal sites at 19 Ma. Accordingly, the Burdigalian transgression in Switzerland most likely had a tectonic driving force, but with amplifications through responses occurring on the surface of the Alps.

References

Allen, J.R.L. : Sedimentary Structures. Their Characteristics and Physical Basis. Vol. I. Developments in Sedimentology 30A. Elsevier, Amsterdam, 593 p., 1982.

Allen, J.R.L. : Sedimentary Structures. Their Characteristics and Physical Basis. Vol. I. Developments in Sedimentology 30B. Elsevier, Amsterdam, 679 p., 1984.

Allen, P.A. : Reconstruction of ancient sea conditions with an example from the Swiss Molasse. Marine Geology 60, 455 – 473, 1984.

Allen, P.A. : Earth Surface Processes, 404 p. ISBN 0-632-03507-2, 1997.

Allen, P. A., and Homewood, P. : Evolution and mechanics of a Miocene tidal sandwave. Sedimentology, 31 (1), 63 – 81, 1984.

Allen, P.A., Mange-Rajetky, A. and Matter, A. : Dynamic palaeogeography of the open Burdigalian seaway, Swiss Molasse basin. Eclogae Geologicae Helvetiae, 78, 351 – 381, 1985.

Allen. P. A. and Bass. J. P. : Sedimentology of the Upper Marine Molasse of the Rhône-Alp region. Eastern France: Implications for basin evolution. Eclogae Geologicae Helvetiae, 86(1), 121 – 171, 1993.

Allen, P. A., Crampton, S. L. and Sinclair, H. D. : The inception and early evolution of the North Alpine foreland basin, Switzerland. Basin Research, 3(3),143 – 163, 1991.

Allen, P.A. and Allen, J.R. : Basin Analysis: Principles and Applications. Malden, MA. Blackwell Pub., ix, 549 p., ISBN: 0632052074, 2005.

Baas, J. H. : Ripple, ripple mark, ripple structure. In: Sedimentology. Encyclopedia of Earth Science, Springer, Berlin, Heidelberg, 921 – 925, 1978.

Bates, C. C. : Rational theory of delta formation. AAPG Bulletin, 37(9), 2119 – 2162, 1953.

Beaumont, C. : Foreland basins. Geophysical Journal International, 65, (2), 291 – 329, 1981.

Berger, J.-P. : Cartes paléogéographiques-palinspastiques du bassin molassique suisse (Oligocène inférieur – Miocène moyen). N. Jb. Geol. Paläont. Abh. 2002 (1), 1 – 44, 1996.

Bieg, U., Süss, M. P., and Kuhlemann, J. : Simulation of tidal flow and circulation patterns in the Early Miocene (Upper Marine Molasse) of the Alpine foreland basin. Analogue and Numerical Modelling of Sedimentary Systems: From Understanding to Prediction, 40, 145 – 169, 2008.

Boston, K.R., Rubatto, J., Hermann, J., Engi, M. and Amelin, Y. : Geochronology of accessory allanite and monazite in the Barrovian metamorphic sequence of the Central Alps, Switzerland. Lithos, 286 – 287, 502 – 518, 2017.

Bridge, J.S. and Tye, R.S. : Interpreting the dimensions of ancient fluvial channel bars, channels and channel belts fromwireline-logs and cores. AAPG Bulletin, 84 (8), 1205 – 1228, 2000.

Burbank, D. W., Engesser, B., Matter, A. and Weidmann, M. : Magnetostratigraphic chronology, mammalian faunas, and stratigraphic evolution of the Lower Freshwater Molasse, Haute-Savoie, France. Eclogae Geologicae Helvetiae, 85(2), 399 – 431, 1992.

Cande, S.C. and Kent, D.V. : A new geomagnetic polarity time scale for the Late Cretaceous and Cenozoic. Journal of geophysical research, 97, 913 – 951, 1992.

Cande, S.C. and Kent, D.V. : Revised calibration of the geomagnetic polarity timescale for the Late Cretacesou and Cenocoic. Journal of geophysical research, 100, 6093 – 6095, 1995.

Cederbom, C.E., Sinclair, H.D., Schlunegger, F. and Rahn, M. : Climate-induced rebound and exhumation of the European Alps. Geology, 32, 709 – 712, 2004.

Cederbom, C.E., van der Beek, P., Schlunegger, F., Sinclair, H.D. and Oncken, O. : Rapid extensive erosion of the North Alpine foreland basin at 5 – 4 Ma. Basin Research, 23(5), 528 – 550, 2011.

Clifton, H.E. and Dingler, J.R. : Wave-Formed Structures and Paleoenvironmental Reconstruction. Marine Geology, 60, 165 – 198, 1984.

Daidu, F., Yuan, W. and Min, L. : Classifications, sedimentary features and facies associations of tidal flats. Journal of Palaeogeography, 2 (1), 66 – 80, 2013.

Dam, G., and Andreasen, F. : High-energy ephemeral stream deltas; an example from the Upper Silurian Holmestrand Formation of the Oslo Region, Norway. Sedimentary Geology, 66 (3-4), 197 – 225, 1990.

Davies, J. and von Blanckenburg, F. : Slab breakoff: A model of lithosphere detachment and its test in the magmatism and deformation of collisional orogens. Earth and Planetary Science Letters, 129, 85 – 102, 1995.

DeCelles, P. G. : Late Jurassic to Eocene evolution of the Cordilleran thrust belt and foreland basin system, western USA. American Journal of Science, 304 (2), 105 – 168, 2004.

DeCelles, P.G. and Giles, K.A. : Foreland basin systems: Basin Research 8, 105 – 123, 1996.

Diem, B. : Analytical method for estimating paleowave climate and water depth from wave ripple marks. Sedimentology, 32, 705 – 720, 1985.

Diem, B. : Die Untere Meeresmolasse zwischen der Saane (Westschweiz) und der Ammer (Oberbayern). Eclogae Geologicae Helvetiae, 79 (2), p. 493 – 559, 1986.

Doppler, G. : Zur Stratigraphie der nördlichen Vorlandmolasse in Bayerisch-Schwaben. Geologica Bavarica, 94, 83 – 133, 1989.

Engesser, B. : Die Eomyidae (Rodentia, Mammalia) der Molasse der Schweiz und Savoyens. Systematik und Biostratigraphie. - Schweiz. Paläont. Abh. 112, 1 – 144, 1990.

Fertig, J., Graf, R., Lohr, H., Mau, J., Müller, M. : Seismic sequence and facies analysis of the Puchkirchen Formation, Molasse basin, south-east Bavaria, Germany. Eur. Assoc. Pet. Geosci. Spec. Publ. 1, 277 – 287, 1991.

Flemings, P. B. and Jordan, T. E. : Stratigraphic modeling of foreland basins: Interpreting thrust deformation and lithosphere rheology. Geology, 18 (5), 430 – 434, 1990.

Flemming, B.W. : Geology, Morphology, and Sedimentology of Estuaries and Coasts. Treatise on Estuaries and Coasts, 3 (2), 7 – 38, 2011.

Frieling, D., Mazumder, R., and Reichenbacher, B. : Tidal sediments in the Upper Marine Molasse (OMM) of the Allgäu area (Lower Miocene, Southwest-Germany). Neues Jahrbuch für Geologie und Paläontologie-Abhandlungen, 254 (1-2), 151 – 163, 2009.

Froitzheim, N., Schmid, S.M. and Frey, M. : Mesozoic paleogeography and the timing of eclogite-facies metamorphism in the Alps: A working hypothesis. Eclogae Geologicae Helvetiae, 89, 81 – 110, 1996.

Fry, B., Deschamps, F., Kissling, E., Stehly, L. and Giardini, D. : Layered azimuthal anisotropy of Rayleigh wave phase velocities in the European Alpine lithosphere inferred from ambient noise. Earth and Planetary Science Letters, 297, 95 – 102, 2010.

Füchtbauer, H. : Sedimentpetrographische Untersuchungen in der älteren Molasse nördlich der Alpen. Eclogae Geologicae Helvetiae, 61, 157 – 298, 1964.

Garefalakis, P. and Schlunegger, F. :. Link between concentrations of sediment flux and deep crustal processes beneath the European Alps. Scientific Reports, 8(1), 183, 2018.

Haldemann, E. G., Haus, H. A., Holliger, A., Liechti, W., Rutsch, R. F., and Della Valle, G. : Geologischer Atlas der Schweiz, Blatt 1188 Eggiwil (Nr. 75): Schweizerische Geologische Kommission, scale 1:25 000, 1 sheet, 1980.

Hammer, B. : Sedimentologie der Oberen Meeresmolasse im Raum St. Gallen. Unpublished Diploma thesis, Univ. Bern, Bern, Switzerland, 96 pp., 1984.

Handy, M.R., Schmid, S.M., Bousquet, R., Kissling, E. and Bernoulli, D. : Reconciling plate-tectonic reconstructions of Alpine Tethys with the geological – geophysical record of spreading and subduction in the Alps. Earth Science Reviews, 102 (3–4), 121 – 158, 2010.

Handy, M.R., Ustaszewski, K. and Kissling, E. :. Reconstructing the Alps-Carpathians-Dinarides as key to understanding switches in subduction polarity, slab gaps and surface motion. International Journal of Earth Sciences, 104 (1), 1 – 26, 2015.

Herwegh, M., Berger, A., Baumberger, R., Wehrens, P. and Kissling, E. : Large-scale crustal-block-extrusion during Late Alpine collision. Scientific Reports 7, 413, 2017.

Hilgen, F. J., Lourens, L. J., Van Dam, J. A., Beu, A. G., Boyes, A. F., Cooper, R. A., Krijgsman, W., Ogg, J.G., Piller, W.E. and Wilson, D. S. : The Neogene period. In: The geologic time scale, 923 – 978, 2012.

Homewood, P. and Allen, P.A. : Wave-, Tide-, and Current-Controlled Sandbodies in Miocene Molasse, Western Switzerland. The American Association of Petroleum Geologists Bulletin 65, 2534 – 2545, 1981.

Homewood, P., Allen, P.A. and Williams, G.D. : Dynamics of the Molasse Basin of western Switzerland. Spec. Publs int. Ass. Sediment., 8, 199 – 217, 1986.

Hurford, A. J. : Cooling and uplift patterns in the Lepontine Alps, south central Switzerland and an age of vertical movement on the Insubric fault line: Contributions to Mineralogy and Petrology, v. 93, 413 – 427, 1986.

Isler, A. and Murer, R. : Geologische Karte der Schweiz, Kartenblatt 1149 Wolhusen 1:25'000, Bundesamt für Landestopographie swisstopo, in press, 2019.

Jin, J., Aigner, T., Luterbacher, H.P., Bachmann, G.H., Müller, M. : Sequence stratigraphy and depositional history in the south-eastern German Molasse Basin. Mar. Pet. Geol. 12, 929 – 940, 1995.

Jordan, T. E. : Thrust loads and foreland basin evolution, Cretaceous, western United States. AAPG bulletin, 65 (12), 2506 – 2520, 1981.

Jordan, T. E. and Flemings, P. B. : Large-scale stratigraphic architecture, eustatic variation, and unsteady tectonism: A theoretical evaluation. Journal of Geophysical Research: Solid Earth, 96 (B4), 6681 – 6699, 1991.

Jost, J., Kempf, O. and Kälin, D. : Stratigraphy and palaeoecology of the Upper Marine Molasse (OMM) of the central Swiss Plateau. Swiss Journal of Geosciences, 109(2), 149 – 69, 2016.

Kälin, D. and Kempf, O. : High-resolution stratigraphy from the continental record of the Middle Miocene Northern Alpine Foreland Basin of Switzerland. N. Jb. Geol. Paläont. Abh., 254, 177 – 235, 2009.

Keller, B. : Fazies und Stratigraphie der Oberen Meeresmolasse (Unteres Miozän) zwischen Napf und Bodensee. Ph.D., Bern, 302 p., 1989.

Keller, B. : Wirkung von Wellen und Gezeiten bei der Ablagerung der Oberen Meeresmolasse–Löwendenkmal und Gletschergarten–zwei anschauliche geologische Studienobjekte. Mitteilungen der Naturforschenden Gesellschaft Luzern, 31, 245 – 271, 1990.

Keller, B. : Facies of Molasse based on a section across the central part of the Swiss Plateau. Swiss Bull. Angew. Geol., 17/2, 3 – 19, 2012.

Keller, B., Bläsi, H.-R., Platt, N.H., Mozley, P.S. and Matter, A. : Sedimentäre Architektur der distalen Unteren Süsswassermolasse und ihre Beziehung zur Diagenese und den petrophysikal. Eigenschaften am Beispiel der Bohrungen Langenthal. - Nagra Technischer Bericht NTB 90-41, Nagra, Wettingen, 1990.

Kempf, O. Bolliger, T., Kälin, D., Engesser, B and Matter, A. : New magnetostratigraphic calibration of Early to Middle Miocene mammal biozones of the North Alpine foreland basin. Mém. Trav. EPHE Inst. Montpellier 21, 547 – 561, 1997.

Kempf, O. : Magnetostratigraphy and facies evolution of the Lower Freshwater Molasse (USM) of eastern Switzerland. Ph.D., Bern, 138 p., 1998.

Kempf, O. and Matter, A. : Magnetostratigraphy and depositional history of the Upper Freshwater Molasse (OSM) of eastern Switzerland. Eclogae Geologicae Helvetiae, 92, 97 – 103, 1999.

Kempf, O., Matter, A., Burbank, D.W. and Mange, M. : Depositional and structural evolution of a foreland basin margin in a magnetostratigraphic framework: the eastern Swiss Molasse basin. International Journal of Earth Sciences, 88, 253 – 275, 1999.

Kissling, E. : Deep structure of the Alps – what do we really know? Physics of the Earth and Planetary Interiors, 79 (1-2), 87 – 112, 1993.

Kissling, E., and Schlunegger, F. : Rollback orogeny model for the evolution of the Swiss Alps. Tectonics, 37(4), 1097 – 1115, 2018.

Kuhlemann, J. : Post-collisional sediment budget of circum-Alpine basins (Central Europe). Mem. Sci. Geol. Padova 52, 1–91, 2000.

Kuhlemann, J., Frisch, W., Dunkl, I., Sze´kely, B., Spiegel, C. : Miocene shifts of the drainage divide in the Alps and their foreland basin. Z. Geomorphol., N.F. 45, 239 – 265, 2001a.

Kuhlemann, J., Frisch, W., Dunkl, I., and Székely, B. : Quantifying tectonic versus erosive denudation by the sediment budget: The Miocene core complexes of the Alps. Tectonophysics, 330(1-2), 1 – 23, 2001b.

Kuhlemann, J., Frisch, W., Székely, B., Dunkl, I., and Kázmér, M. : Post-collisional sediment budget history of the Alps: tectonic versus climatic control. International Journal of Earth Sciences, 91(5), 818 – 837, 2002.

Kuhlemann, J. and Kempf, O. : Post-Eocene evolution of the North Alpine Foreland Basin and its response to Alpine tectonics. Sedimentary Geology 152, 45 – 78, 2002.

Kühni, A. and Pfiffner, O. A. : The relief of the Swiss Alps and adjacent areas and its relation to lithology and structure: topographic analysis from a 250-m DEM. Geomorphology, 41(4), 285 – 307, 2001.

Leclair, S.F. and Bridge, J.S. : Quantitative interpretation of sedimentary structures formed by river dunes. Journal of Sedimentary Research, 71, 713 – 716, 2001.

Lemcke, K., Engelhardt, W. V., and Füchtbauer, H. : Geologische und sedimentpetrographische Untersuchungen im-Westteil der ungefalteten Molasse des süddeutschen-Alpenvorlandes. Beihefte zum Geologischen Jahrbuch, 11, 1 – 182, 1953.

Lihou, J.C, and Allen, P.A. : Importance of inherited rift margin structures in the early North Alpine Foreland Basin, Switzerland. Basin Research, 8, 425 – 442, 1996.

Lippitsch, R., Kissling, E. and Ansorge, J. : Upper mantle structure beneath the Alpine orogen from high-resolution teleseismic tomography. Journal of Geophysical Research, 108(B8), 2376, 2003.

Lourens, L. J., F.J. Hilgen, J. Laskar, Shackleton, N. J., and Wilson, D. : The Neogene Period. A Geologic Time Scale 2004, Cambridge University Press, 409 – 440, 2004.

Lu, G., Winkler, W., Rahn, M., von Quadt, A. and Willett, S.D. : Evaluating igneous sources of the Taveyannaz formation in the Central Alps by detrital zircon U–Pb age dating and geochemistry. Swiss Journal of Geosciences, 111(3), 399 – 416, 2018.

Malzer, O., Rögl, F., Seifert, P., Wagner, L., Wessely, G., Brix, F. : Die Molassezone und deren Untergrund. Erdöl und Erdgas in Österreich, 281 – 322, 1993.

Mancktelow, N. : The Simplon Line: a major displacement zone in the western Lepontine Alps. Eclogae Geologicae Helvetiae, 78(1), 73 – 96, 1985.

Mancktelow, N. S., and Grasemann, B. : Time-dependent effects of heat advection and topography on cooling histories during erosion. Tectonophysics, 270 (3-4), 167 – 195, 1997.

Matter, A. : Sedimentologische Untersuchungen im östlichen Napfgebiet (Entlebuch – Tal der Grossen Fontanne, Kt. Luzern). Eclogae Geologicae Helvetiae, 57, 315 – 429, 1964.

Matter, A., Homewood, P., Caron, C., Rigassi, D., van Stuijvenberg, J., Weidmann, M. and Winkler, W. : Flysch and Molasse of western and central Switzerland. Exc. Guidebook No. 126A 26th Int. Geol. Congr. Schweiz. Geol. Komm. Wepf and Co. Publ., Basel, 1980.

Mazurek M, Hurford A, Leu W. : Unravelling the multi-stage burial history of the Swiss Molasse basin: Integration of Apatite fission track, vitrinite reflectance and biomarker isomerisation analysis. Basin Research, 18, 27 – 50, 2006.

Mein, P. : Résultats du groupe de travail des vertébrés: Biozonation du Néogène méditerranéen à partir des Mammifères. In: Sénès, J. (ed.), Report Report on Activity of the RCMNS Working groups (1971-1975), 78 – 81, Bratislava, 1975.

Mein, P. : Rapport d'activité du Groupe de Travail Vertébrés Mise à jour de la biostratigraphie du Néogène basée sur les Mammifères. Ann. géol. Pays Héilen., Tome hors série, 3, 1367-72. (VII International Congress on Mediterranean Neogene, Athens, 1979), 1979.

Mein, P. : Updating of MN zones. In: Lindsay. E., Fahlbusch, V. and Mein. P. (eds.), European Neogene mammal chronology. NATO ASI, Life Sci. 180, 73 – 90. Plenum Press, New York, 1989.

Mey, J., Scherler, D., Wicker, A., Egholm, D., Tesauro, M., Schildgen, T.F., and Strecker, M. : Glacial isostatic uplift of the European Alps. Nature Communications, 7, 13382, 2016.

Miall, A.D. : Lithofacies types and vertical profile models in braided river deposits, a summary. In: MIALL, A.D. (Ed.): Fluvial sedi- mentology. p. 597-604. -Can. Soc. Petr. Geol. Mem. 5, 1978.

Miall, A.D. : Architectural-Element Analysis : A New Method of Facies Analysis Applied to Fluvial Deposits. Earth-Sci. Rev. 22, 261 – 308, 1985.

Miall, A. D. : The Geology of Fluvial Deposits. Sedimentary Facies, Basin Analysis, and Petroleum Geology. Springer. 582 p., 1996.

Miller, M.C. and Komar, P.D. : Oscillation Sand Ripples Generated by Laboratory Apparatus. Journal of Sedimentary Research, 50(1), 173 – 182, 1980a.

Miller, M.C. and Komar, P.D. : A field investigation of the relationship between oscillation ripple spacinng and the near-bottom water orbital motions. Journal of Sedimentary Research, 50 (1), pp.183 – 191, 1980b.

Miller, K.G., Mountain, G.S., the Leg 150 Shipboard Party, and Members of the New Jersey Coastal Plain Drilling Project : Drilling and dating New Jersey Oligocene–Miocene sequences: Ice volume, global sea level, and Exxon records. Science 271(1), 92 – 94, 1996.

Miller, K.G., Mountain, G.S., Browning, J.V., Kominz, M., Sugarman, P.J., Christie-Blick, N., Katz, M.E. and Wright, J.D. : Cenozoic global sea level, sequences, and the New Jersey transect: results from coastal plain and continental slope drilling. Rev. Geophys., 36, 569 – 601, 1998.

Nichols, P.G. : Sedimentology & Stratigraphy. Blackwell Sci., 355 p., 1999.

Ortner, H., Fügenschuh, B., Zerlauth, M., Hinsch, R., Friedrich, A., Hofmann, F., and Neumeier, G. : Geometry, sequence and amount of thrusting in the sub-Alpine Molasse of Austria and Bavaria. Fragile Earth: Geological processes from global to local scales and associated hazards: Boulder, Geological Society of America A, 39, 2011.

Pippèrr, M. and Reichenbacher, B. : Late Early Miocene palaeoenvironmental changes in the North Alpine Foreland Basin. Palaeogeography, Palaeoclimatology, Palaeoecology 468, 485 – 502, 2017.

Pfiffner, O.A. : Evolution of the north Alpine foreland basin in the Central Alps. Special Publication, International Association of Sedimentologists 8, 219 – 228, 1986.

Pfiffner, O. A., Schlunegger, F. and Buiter, S. J. H. : The Swiss Alps and their peripheral foreland basin: Stratigraphic response to deep crustal processes. Tectonics, 21(2), 2002.

Platt, N. H. and Keller, B. : Distal alluvial deposits in a foreland basin setting—the Lower Freshwater Miocene), Switzerland: sedimentology, architecture and palaeosols. Sedimentology, 39 (4), 545 – 565, 1992.

Python, C. : Geologische Karte der Schweiz, Kartenblatt 1185 Fribourg 1:25’000, Bundesamt für Landestopographie swisstopo, 1996.

Reichenbacher, B., Krijgsman, W., Lataster, Y., Pipperr, M., Van Baak, C. G., Chang, L., Kälin, D., Jost, J., Doppler, G., Jung, D., Priet, J., Abdul Aziz, H., Böhme, M., Garnish, J., Kirscher, U. and Bachtadse, V. : A new magnetostratigraphic framework for the Lower Miocene (Burdigalian/Ottnangian, Karpatian) in the North Alpine Foreland Basin. Swiss Journal of Geosciences, 106(2), 309 – 334, 2013.

Reichenwallner, S. : Die vulkanische Aktivität in den Westalpen hergeleitet aus detritischem Amphibol und Klinopyroxen im Taveyannaz-Sandstein. Unpublished Ms-thesis, University of Bern, Bern, 57 pp. 2019.

Reineck, H.E. and Singh, I. B. : Depositional sedimentary environments. Springer, 549 p., 1980.

Rust, B.R. and Gibling, M.R. : Braidplain evolution in the Pennsylvanian South Bar Formation, Sydney basin, Noca Scotia, Canada. Journal of Sedimentary Petrology, 60 (1), 59 – 72, 1990.

Salvermoser, S. Zur Sedimentologie gezeiten-beeinflusster Sande in der Oberen Meeresmolasse und Süssbrackwassermolasse (Ottnangium) von Niederbayern und Oberösterreich. Münchner Geologische Hefte, A, 26: 1 – 179, 1999.

Sant, K., V. Palcu, D., Mandic, O., and Krijgsman, W. : Changing seas in the Early–Middle Miocene of Central Europe: a Mediterranean approach to Paratethyan stratigraphy. Terra Nova, 29(5), 273 – 281, 2017.

Schaad, W., Keller, B. and Matter, A. : Die Obere Meeresmolasse (OMM) am Pfänder: Beispiel eines Gilbert-Deltakomplexes. Eclogae Geologicae Helvetiae, 85, 145 – 168, 1992.

Shanmugam, G. : Deep-marine tidal bottom currents and their reworked sands in modern and ancient submarine canyons. Marine and Petroleum Geology, 20 (5), 471 – 491, 2003.

Schlunegger, F., Burbank, D.W., Matter, A., Engesser, B. and Mödden, C. : Magnetostratigraphic calibration of the Oligocene to Middle Miocene (30–15 Ma) mammal biozones and depositional sequences of the Swiss Molasse Basin. Eclogae Geologicae Helvetiae, 89, 753 – 788, 1996.

Schlunegger, F., Leu, W. and Matter, A. : Sedimentary Sequences, Seismic Facies, Subsidence Analysis, and Evolution of the Burdigalian Upper Marine Molasse Group, Central Switzerland. The American Association of Petroleum Geologists 81, 1185 – 1207, 1997a.

Schlunegger, F., Jordan, T.E., and Klaper, E.M. : Controls of erosional denudation on foreland basin evolution: The Oligocene central Swiss Molasse Basin as an example. Tectonics, 16, 823 – 840, 1997b.

Schlunegger, F., Slingerland, R. and Matter, A. : Crustal thickening and crustal extension as controls on the evolution of the drainage network of the central Swiss Alps between 30 Ma and the present: constraints from the stratigraphy of the North Alpine Foreland Basin and the structural evolution of the Alps. Basin Research, 86, 717 – 750, 1998.

Schlunegger, F. and Willett, S. : Spatial and temporal variations in exhumation of the central Swiss Alps and implications for exhumation mechanisms. Geological Society, London, Special Publications, 154(1), 157 – 179, 1999.

Schlunegger, F. and Hinderer, M. : Crustal uplift in the Alps: why the drainage pattern matters. Terra Nova, 13(6), 425 – 432, 2001.

Schlunegger, F., and Kissling, E. : Slab rollback orogeny in the Alps and evolution of the Swiss Molasse basin. Nature Communications, 6, 8605, 2015.

Schlunegger, F., Anspach, O., Bieri, B., Böning, P., Kaufmann, Y., Lahl, K., Lonschinski, M., Mollet, H., Sachse, D., Schubert, C., Stöckli, G. and Zander, I. : Geologische Karte der Schweiz, Kartenblatt 1169 Schüpfheim 1:25'000, Bundesamt für Landestopographie swisstopo, 2016.

Schlunegger, F. and Castelltort, S. : Immediate and delayed signal of slab breakoff in Oligo / Miocene Molasse deposits from the European Alps. Scientific Reports, 6, 31010, 2016.

Schmid, S. M., Pfiffner, O. A., Froitzheim, N., Schönborn, G., and Kissling, E. : Geophysical-geological transect and tectonic evolution of the Swiss-Italian Alps. Tectonics, *15*(5), 1036 – 1064, 1996.

Schmid, S. M., Fügenschuh, B., Kissling, E. and Schuster, R. : Tectonic map and overall architecture of the Alpine orogen. Eclogae Geologicae Helvetiae, 97(1), 93 – 117, 2004.

Short, A. D. : Coastal Processes and Beaches. Nature Education Knowledge 3(10): 15, 2012.

Sinclair, H.D., Coakley, B.J., Allen, P.A. and Watts, A.B. : Simulation of foreland basin stratigraphy using a diffusion model of mountain belt uplift and erosion: An example from the Central Alps, Switzerland. Tectonics 10, 599 – 620, 1991.

Sinclair, H.D. and Allen, P.A. : Vertical versus horizontal motions in the Alpine orogenic wedge: stratigraphic response in the foreland basin. Basin Research 4, 215 – 232, 1992.

Sinclair, H. D. : Plan-view curvature of foreland basins and its implications for the palaeostrength of the lithosphere underlying the western Alps. Basin Research 8.2, 173-182, 1996.

Strunck, P. and Matter, A. : Depositional evolution of the western Swiss Molasse. Eclogae Geologicae Helvetiae, 95, 197 – 222, 2002.

Tesauro, M., Kaban, M.K. and Cloething, S.A.P.L. : Global model for the lithospheric strength and effective elastic thickness:. Tectonophysics 602, 78 – 86, 2013.

Tesauro, M., Kaban, M.K. and Cloething, S.A.P.L. : How rigid is Europe's lithosphere? Geophys. Res. Lett. 36, 1 – 6, 2009.

Ustaszewski, K., Schmid, S.M, Fügenschuh, B., Tischler, M., Kissling, E. and Spakman, W. : A map-view restoration of the Alpine-Carpathian-Dinaridic system for the Early Miocene. Swiss Journal of Geosciences, 101 (SUPPL. 1), 273 – 294, 2008.

Waschbusch, P.J., and Royden, L.H. : Spatial and temporal evolution of foredeep basins: lateral strength variations and inelastic yielding in continental lithosphere. Basin Research, 4, 179 – 196, 1992.

Wanner, J., Gisler, C., Jost, J., Christener, F. Ninck, T. : Geologische Karte der Schweiz, Kartenblatt 1148 Sumiswald 1:25'000, Bundesamt für Landestopographie swisstopo, in press, 2019.

Wehrens, P. : Structural evolution in the Aar Massif (HaslitaI transect): Implications for midcrustal deformation. Ph.D., Bern, 2015.

Wehrens, P., Baumberger, R., Berger, A. and Herwegh, M. : How is strain localized in a meta-granitoid, mid-crustal basement section? Spatial distribution of deformation in the central Aar massif (Switzerland), Journal of Structural Geology, 94, 47 – 67, 2017.

Willett, S. D. : Late Neogene erosion of the Alps: A climate driver?. Annual Review of Earth and Planetary Sciences, 38, 411-437, 2010.

Yalin, M.S. : Geometrical properties of sand waves. Journal of the Hydraulics Division, ASCE, 90, 105 – 119, 1964.

Zachos, J., Pagani, M., Sloan, L. Thomas, E. and Billups, K. : Trends, rhythms and aberrations in global climate 65 Ma to present, Science, 292, 686 – 693, 2001.

Author contribution

F.S. designed the study. P.G. carried out the experiments, collected and interpreted the data with support by F.S.. The figures and photos were done/taken by P.G. with support by F.S. F.S. and P.G. wrote the text."

Competing interest

The authors declare that they have no conflict of interest.

Tables and Figures

Table 1: Lithofacies encountered in the Entlen section

Facies assemblages	*Structures and Bedforms*	*Depositional setting & references*
Mcl, Mm, Mp, Mfl, Mle	Climbing ripples (Mcl), mudstone drapes (Md) and flaser- (Mfl) and lenticular-bedding (Mle) within parallel-laminated (Mp) and massive-bedded mudstones (Mm)	Wave-dominated environment: Backshore setting, where sediments were deposited within a swampy area. Root-casts, reddish mottling and caliche nodules represent palaeo-sol formation. *Keller, 1989; Miall, 1996 ; Daidu et al., 2013*
Md, Mfl, Mle,	Mudstone drapes (Md), flaser- (Mfl) and lenticular-bedding (Mle)	Wave-dominated environment with strong tidal influence: Backshore to nearshore setting, where Mle mostly form in the supratidal (mudflat) and Mfl form in the intertidal (sandflat) or alternatively in the subtidal, if ripple crests are fully preserved. *Keller, 1989 ; Shanmugam, 2003; Daidu et al., 2013*
Sct_r, Sct_a, Scr	Trough- and tabular-cross-beds (Sct_r, Sct_a) superimposed by current-ripple marks (Scr) which record an opposite flow direction.	Wave-dominated environment with strong tidal influence: Nearshore setting, deposits of (subtidal) sanddunes and sandwaves. *Baas, 1978; Allen and Homewood, 1984; Jost et al., 2016*
Sg, Shf, Sm, Sp, Sv	Pebbly-lags (Sg), Shell-fragments (Shf) within massive- to parallel-laminated sandstones (Sm, Sp), occasionally with sand-volcanoes (Sv)	Wave-dominated environment: Foreshore to nearshore setting within the beach area, deposited at the surf-and-swash zone. *Allen et al., 1985; Dam and Andreasen, 1990; Keller, 1990; Miall, 1996; Jost et al., 2016*
Sbr, Scr, Sos, Sc, Sm, Sp	Ripple marks (Sbr, Scr, Sos) and cross-beds (Sc) within massive-bedded and parallel-laminated sandstones (Sm, Sp)	Wave-dominated environment: Nearshore to foreshore setting, where ripple marks form at the wave area, while Sp form at the surf-and-swash zone (beach area) *Baas, 1978; Reineck and Singh, 1980; Clifton and Dingler, 1984; Allen, J. 1984; Keller, 1989; 1990*
Spw, Sc, Sos, Sm	Sandstone beds with a planar base and a wavy top (Spw) internally cross-bedded (Sc), superimposed by oscillation-ripple marks (Sos) within massive-bedded sandstones (Sm)	Wave-dominated environment: Nearshore to offshore setting, high-energetic storm deposits (tempestites) *Allen, J., 1982; 1984; Clifton and Dingler, 1984; Miller and Komar, 1980a; 1980b; Diem, 1986; Rust and Gibling, 1990*

Table 2: Lithofacies encountered in the Napf units

Facies assemblages	*Structures and Bedforms*	*Depositional setting & references*
Gc, Gm	Cross- (Gc) and massive-bedded (Gm) conglomerates	Fluvial-dominated environment: megafan deposits within a braided river system. Gm, Gc form in active channels. *Platt and Keller, 1992; Schlunegger et al., 1997*
Sc, Sm, Mp	Cross- (Sc) and massive-bedded (Sm) sandstones with parallel-laminated mudstones (Mp)	Fluvial-dominated environment: megafan deposits within a braided river system. Sc, Sm from crevasse-splay deposits. Mp (often yellowish-reddish mottled with caliche nodules and root casts) are evident for palaeo-sol genesis on a floodplain. *Allen, J., 1982; 1984; Rust and Gibling, 1990; Dam and Andreasen, 1990; Keller, 1990*

Table 3: Lithofacies encountered in the Sense section

Facies assemblages	*Structures and Bedforms*	*Depositional setting & references*
Gm, Gc	Massive- to cross-bedded conglomerates (Gm, Gc)	Fluvial-dominated environment: Terrestrial setting, where coarse-grained rivers deposited material. *Platt and Keller, 1992; Schlunegger et al., 1997*
Sc, Sg, Sct_r, Sm	Cross-bedded sandstones (Sc) with top-, fore- and bottom-sets with pebbly lags (Sg) and within trough-cross- (Sct_r) and massive-bedded sandstones (Sm)	Fluvial-dominated environment with tidal influence: Foreshore setting, where deltas, or alternatively estuaries, enter the sea: Sc and Sg mark Gilbert-Delta-type deposits, while Sct_r and Sm mark mouth bar deposits (or alternatively: sanddunes). *Allen, J., 1982; 1984; Allen and Homewood, 1984; Rust and Gibling, 1990; Dam and Andreasen, 1990*
Gm, Gc, Mm, Sm, Sg	Massive- to cross-bedded conglomerates (Gm, Gc) within massive-bedded sand- and mudstones (Sm, Mm). Occasionally, pebbles only occur as isolated layers (Sg)	Tidal-dominated environment with fluvial influence (river inflow): Nearshore setting. Terrestrial derived material washed into subtidal by high energetic floods. *Dam and Andreasen, 1990; Platt and Keller, 1992; Miall, 1996; Schlunegger et al., 1997*
Mm, Mp, Mf	Massive-bedded (Mm) and parallel-laminated (Mp) mudstones with bioturbation (Mf)	Tidal-dominated environment: Backshore setting, deposits of the supratidal (mudflat). *Dan and Andreasen, 1990; Keller, 1990; Miall, 1996*
Sm, Mm, Mf, Sf	Strongly bioturbated (Mf, Sf) massive-mud- and sandstones (Mm, Sm)	Tidal-dominated environment: Backshore to foreshore setting, deposits of mud- (supratidal) and sandflats (intertidal) *Dan and Andreasen, 1990; Keller, 1990; Miall, 1996; Nichols, 1999*
Scr, Md, Sct_a, Sf	Current-ripples (Scr) and tabular cross-beds (Sct_a) with mudstone drapes (Md), occasionally with heavily bioturbated sandstones (Sf)	Tidal-dominated environment: Foreshore setting, deposits of the intertidal (sandflat), where bioturbation occurs (Sf). Mudstone drapes record slack-water phases. *Baas, 1978; Reineck and Singh, 1980; Allen and Homewood, 1984; Shanmugam, 2003; Nichols, 1999*
Sc, Sce	Cross-bedded (Sc) sandstones, occasionally forming epsilon cross-beds (Sce)	Tidal-dominated environment: Foreshore to nearshore setting, deposits of a (meandering) tidal channel. *Allen, J., 1982; 1984; Frieling et al., 2009*
Sos, Sbr, Sp	Oscillation- and branching-ripple marks that grade into parallel-laminated sandstones	Tidal-dominated environment with strong wave influence: Foreshore to nearshore setting, deposits of the beach area (surf-and-swash zone) and the wave-transformation area. *Reineck and Singh, 1980; Clifton and Dingler, 1984; Allen, J. 1984; Keller, 1990*
Sct_a, Scr, Md, Sct_r, Sm	Tabular- (Sct_a) and trough-cross-bedded (Sct_r) sandstones, superimposed with current-ripples (Scr) and mudstone drapes (Md) within massive-bedded sandstones (Sm)	Tidal-dominated environment with fluvial influence (river inflow): Foreshore to nearshore environment. Estuaries (Sct_a, Scr, Md) entering the sea, building up mouth-bar deposits or alternatively subtidal sanddunes (Sct_r, Sm).

		Yalin, 1964; Baas, 1978; Allen and Homewood, 1984; Dam and Andreasen, 1990; Jost et al., 2016
Sct_r, Scr, Md	Trough-cross-beds (Sct_r) superimposed by current-ripple marks (Scr) and mudstone drapes (Md)	Tidal-dominated environment: Nearshore setting, deposits of (subtidal) sanddunes and sandwaves. *Baas, 1978; Allen and Homewood, 1984; Shanmugam, 2003; Jost et al., 2016.*
Spw, Sos, Sg	Sandstone beds with a planar base and a wavy top (Spw), superimposed by oscillation-ripple marks (Sos) and embedded with pebbles (Sg)	Tidal-dominated environment with wave influence: Nearshore to offshore setting, high-energetic storm deposits (tempestites) *Reineck and Singh, 1980; Miller and Komar, 1980a; 1980b; Clifton and Dingler, 1984; Diem 1986; Miall, 1996*

Table 4: Lithofacies encountered at the St. Magdalena site & Gurten drill core

Facies assemblages	***Structures and Bedforms***	***Depositional setting & references***
Sct_r, Scr, Sc, Sm Md	Trough-cross-beds (Sct_r) and cross-bedded sandstones (Sc) superimposed by current-ripple marks (Scr) and mudstone drapes (Md), often within massive-bedded sandstones (Sm)	Tidal-dominated environment: Nearshore setting, deposits of (subtidal) sanddunes (or mouth-bar deposits) and megaripples, We infer these deposits as sediments of subtidal shoals. *Baas, 1978; Allen, J., 1982; 1984; Allen and Homewood, 1984; Rust and Gibling, 1990; Dam and Andreasen, 1990; Shanmugam, 2003*

Table 5: Lithofacies encountered in the Lake Neuchâtel and Wohlen areas

Facies assemblages	***Structures and Bedforms***	***Depositional setting & references***
Scc, Sc, Scr, Shf, Sg	Calcareous, shelly-sandstones (Scc; "Muschelsandstein") are made up of cross-bedded sandstones (Sc), contain coquinas and shell-fragments (Shf) and pebbles (Sg) in places.	Tidal-dominated environment: Offshore setting, mega-sandwaves deposited under strong tidal-currents. Pebbly lags (Sg) are interpreted as pebbles flushed into the sea by flood-events. *Baas, 1978 ; Allen et al., 1985; Rust and Gibling, 1990 ; Miall, 1996 ; Jost et al., 2016*
Sct_a, Sct_r, Slc	Coarse-grained sandstones (Slc, "Grobsandstein") with trough (Sct_r) and tabular (Sct_a) cross-bedded geometries.	Tidal-dominated environment: Nearshore to offshore setting, sandwaves, or alternatively sanddunes, similar to the subtidal-shoal deposits (see St. Magdalena site), however larger in diameters, but similar thicknesses. *Allen and Homewood, 1984; Jost et al., 2016*

(a)

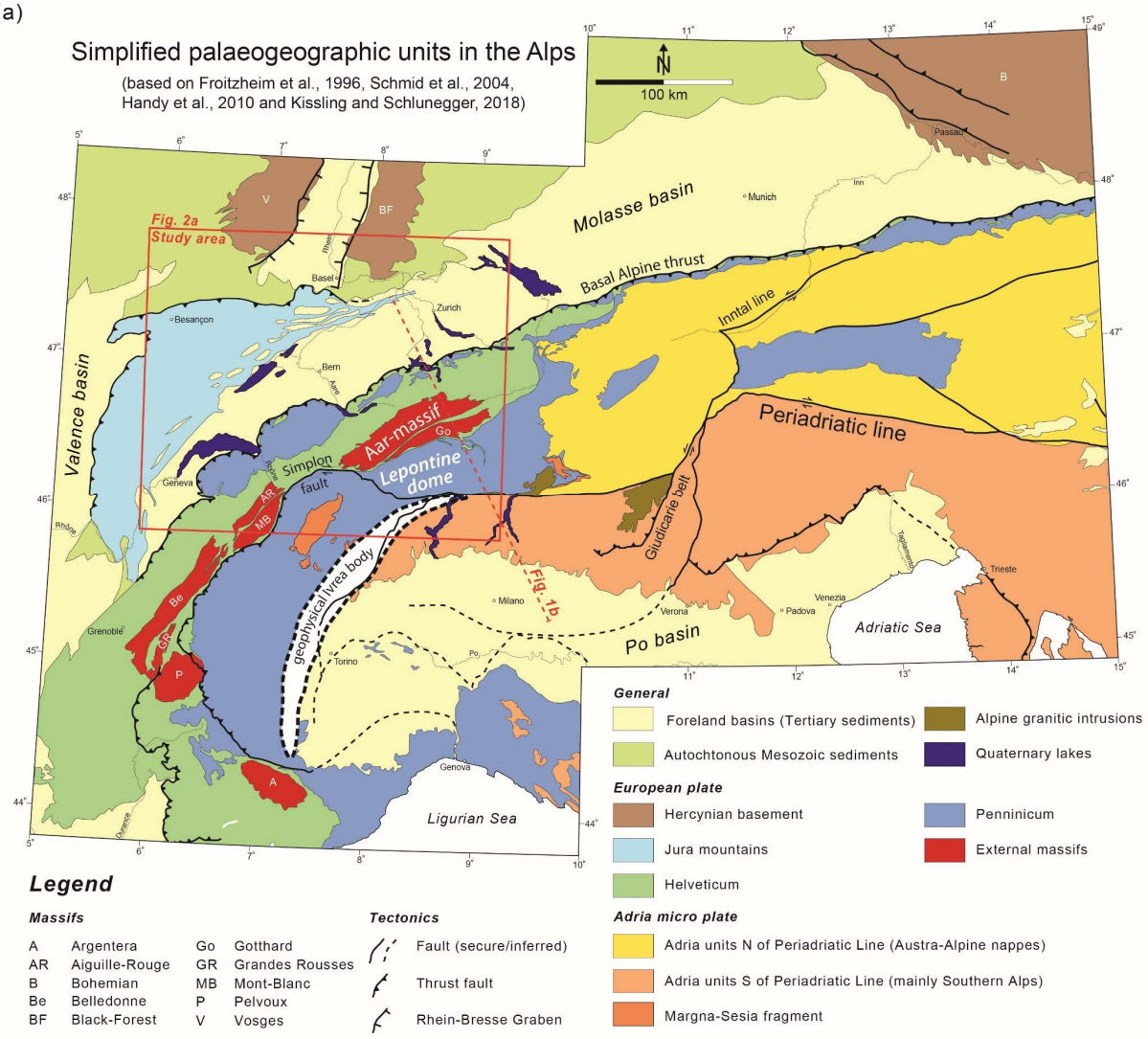

General

- Foreland basins (Tertiary sediments)
- Autochtonous Mesozoic sediments
- Alpine granitic intrusions
- Quaternary lakes

European plate

- Hercynian basement
- Jura mountains
- Helveticum
- Penninicum
- External massifs

Adria micro plate

- Adria units N of Periadriatic Line (Austra-Alpine nappes)
- Adria units S of Periadriatic Line (mainly Southern Alps)
- Margna-Sesia fragment

Legend

Massifs

A	Argentera	Go	Gotthard
AR	Aiguille-Rouge	GR	Grandes Rousses
B	Bohemian	MB	Mont-Blanc
Be	Belledonne	P	Pelvoux
BF	Black-Forest	V	Vosges

Tectonics

- Fault (secure/inferred)
- Thrust fault
- Rhein-Bresse Graben

(b)

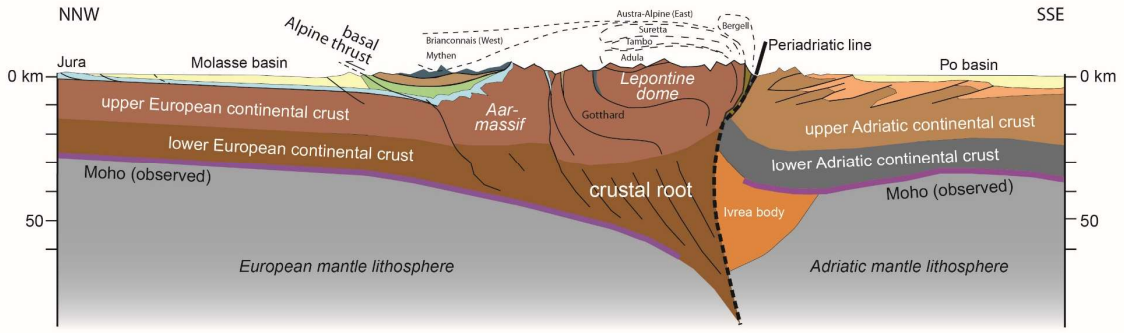

- Flysch
- Helvetic nappes
- Mesozoic-Cenozoic sedimentary rocks of the European plate
- Mesozoic sedimentary cover of the Adriatic plate

Figure 1: a) Simplified geological map of the European Alps based on the compilation by Kissling and Schlunegger (2018) and updated using additional information from Handy et al. (2015) and Pippèrr and Reichenbacher (2017); **b)** Simplified geological-geophysical section through the central European Alps adapted from Kissling and Schlunegger (2018). Note location of Fig. 2a.

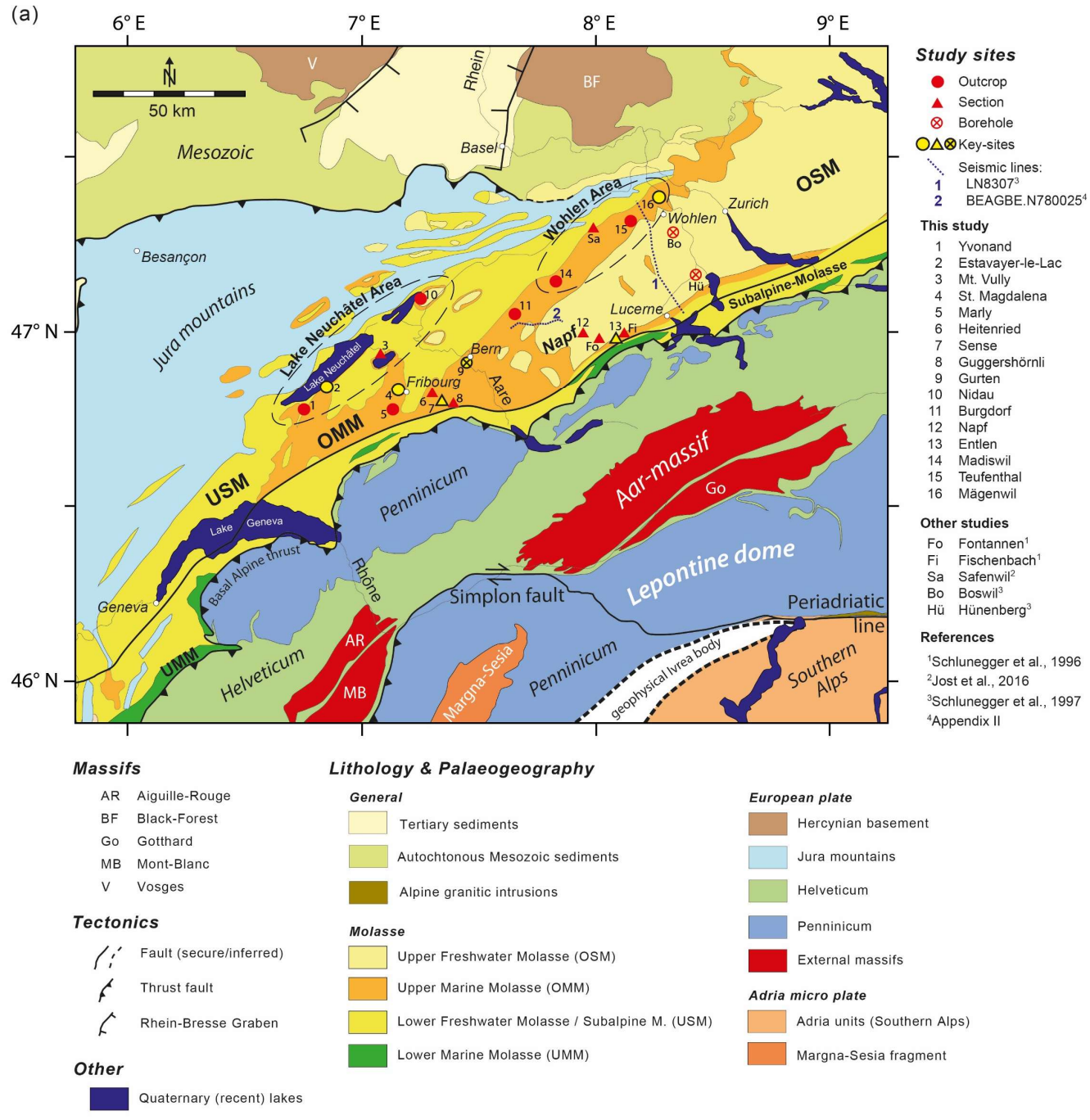

Map mod. after Froitzheim et al., 1996; Schmid et al., 2004; Handy et al., 2010 and Kissling and Schlunegger, 2018

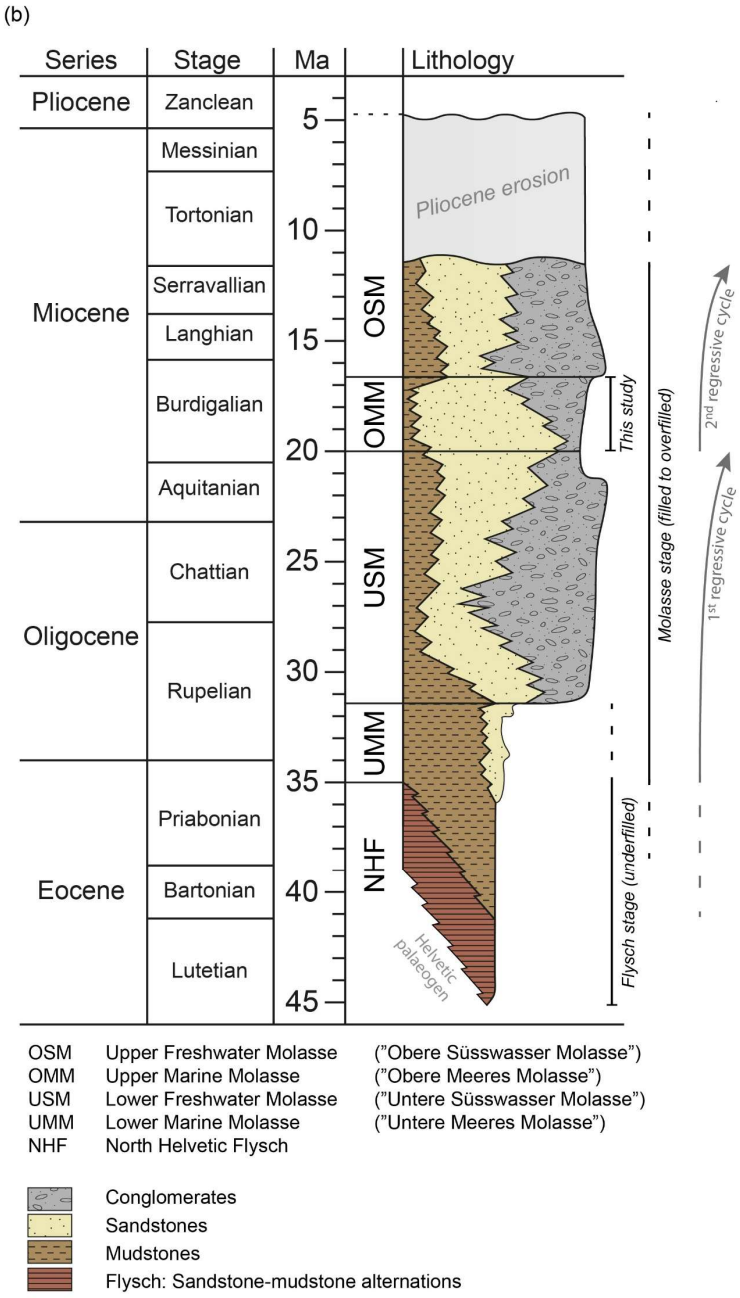

Figure 2: a) Detailed geological map of the area between Geneva and Zurich adapted from Kissling and Schlunegger (2018) showing the locations of data points referred to in this paper. The OMM deposits at sites 1 to 16 have been mapped at the scale of 1:25'000, which was used to reproduce Fig. 6. In addition, the observations of the sections outcrops and the drill core at sites 2, 4, 7, 9, 12, 13 and 16 are explicitly described in chapters 4 and 5 of this paper. Please refer to Fig. 1 for the complete legend. **b**) Lithostratigraphic scheme of the Molasse deposits in Switzerland. Modified after Keller (1989).

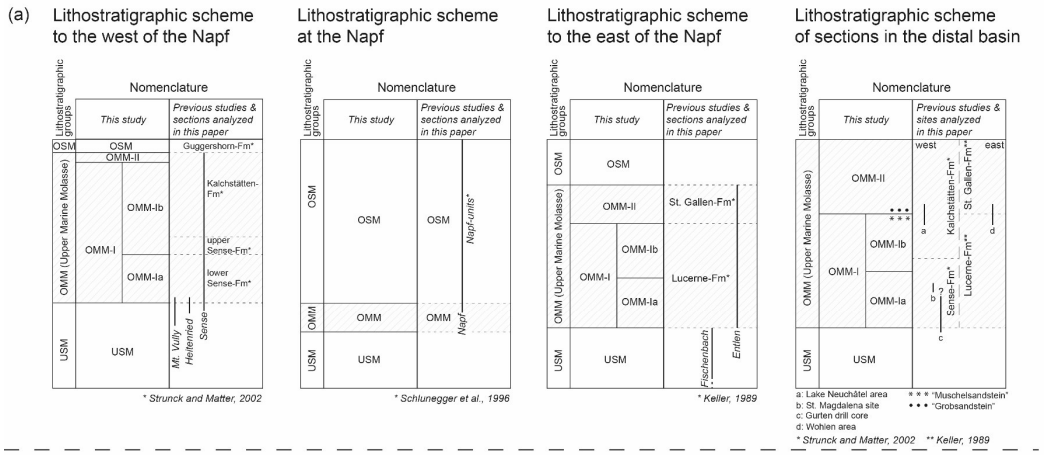

(b)

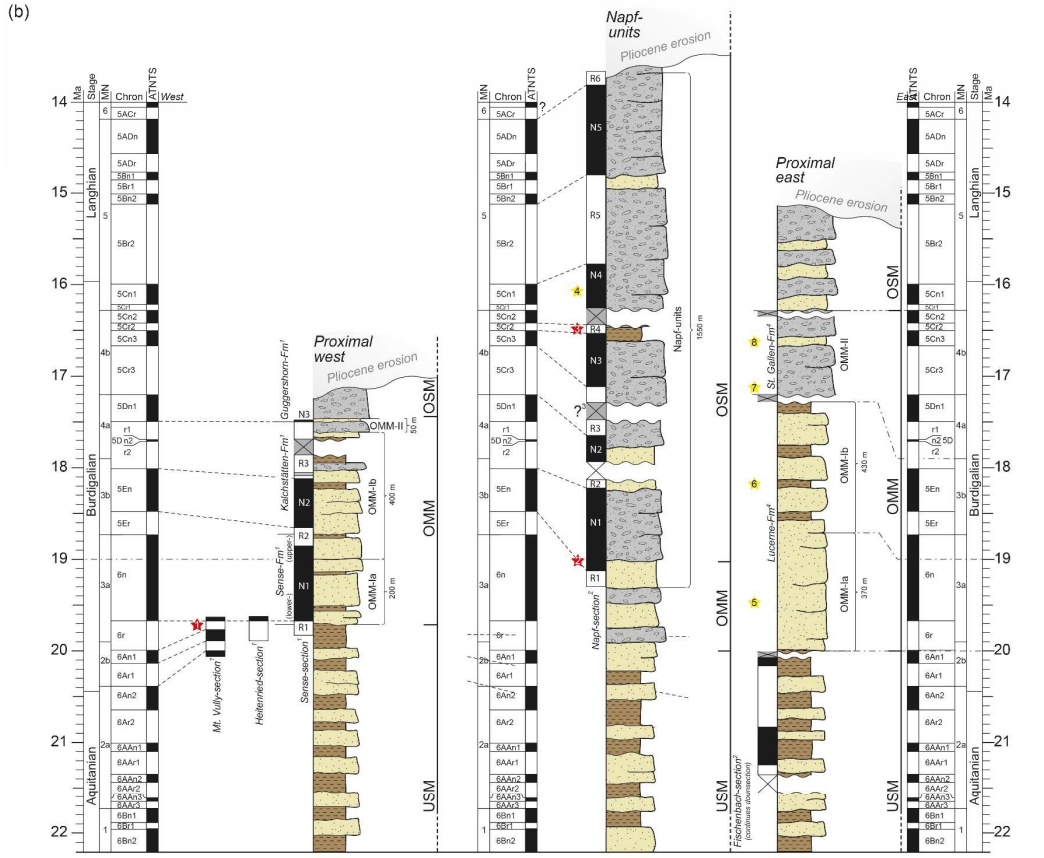

Legend

Section thickness

c. 100 m

Magnetic polarity stratigraphies

- Hiatus mapped
- Hiatus inferred
- Normal polarity
- Reverse polarity
- Discarded magnetozone

ATNTS = astronomically tuned Neogene time - scale[5]

Lithologies

Conglomerates
Sandstones
Mudstones

Mammal zonation

MN = European Neogene mammal (MN) units[6]

MN1/2a and MN5/6	after Hilgen et al., 2012
MN2a/2b	after Strunck and Matter, 2002
MN2b/3a	after Kälin and Kempf, 2009
MN3a/3b and 4a/5	after Sant et al., 2017
MN3b/4a	after Keller, 1989 and after Strunck and Matter, 2002
MN4a/4b	after Jost et al., 2016

Mammalian sites (in-situ)

- = Vully 1; MN2b[1]
- = Hasenbach 1; MN3b[2] or lower MN3b[3]
- = Eimättli in "basal marls"; MN4b[2,3]

Mammalian sites (projected)

- 4 = Oeschgraben; upper/middle MN5[3]
- 5 = Lu 10/76; MN3 or younger[4]
- 6 = Hi 2/6; MN3b[4]
- 7 = Halten; MN4a or MN4b[4]
- 8 = Sitter; MN4 or younger[4]

References

[1]Strunck and Matter, 2002
[2]Schlunegger et al., 1996
[3]Kälin and Kempf, 2009
[4]Keller, 1989
[5]Lourens et al., 2004
[6]Mein, 1975; 1979; 1989

Figure 3: a) Lithostratigraphic scheme of the OMM in Switzerland. **b)** Composite stratigraphic columns illustrating sedimentary architectures at the proximal basin border in the western Molasse basin (proximal west), in the central part of the Molasse basin (Napf units) and in the eastern basin (proximal east). The composite section for the proximal west basin is based on data from the Mt. Vully- and Heitenried-sections, drillings, and from surface information from the Sense-section (Sense beds and Kalchstätten Formation) (Strunck and Matter, 2002). The composite section representative of the central part of the Molasse Basin (Napf) is mainly based on the sedimentary logs by Schlunegger et al. (1996; see their Schwändigraben- and Fontannen-sections) complemented with information from the geological map of the region (Schlunegger et al., 2016). Note that Kälin and Kempf (2009) proposed a very short hiatus recorded by magnetozone R3 within the Napf-units which we do not discuss in detail for simplicity purposes. The composite section illustrating the situation at the proximal basin border east of the Napf represents the sedimentary architecture as far east as of Lake Zurich (Fig. 2a). It is based on data from Keller (1989, see his Rümlig-, Ränggloch- and Lucerne-sections) and from Schlunegger et al., (1996, see their Fischenbach-section) and geological maps of the region (Wolhusen; Isler and Murer, 2019). Note that the Entlen section is situated immediately east of the Napf (Fig. 5a) where the lowermost part (Lucerne Formation) can be characterized by the composite section of the proximal east, whereas the topmost part is made up of conglomerates of the Napf units. Detailed sedimentological data of the Sense-Formation and the Lucerne Formation are shown in Fig. 4. Note that the Molasse units shown in capitals (i.e. USM, OMM and OSM) are based on lithological architecture and thus on facies associations identified in the field.

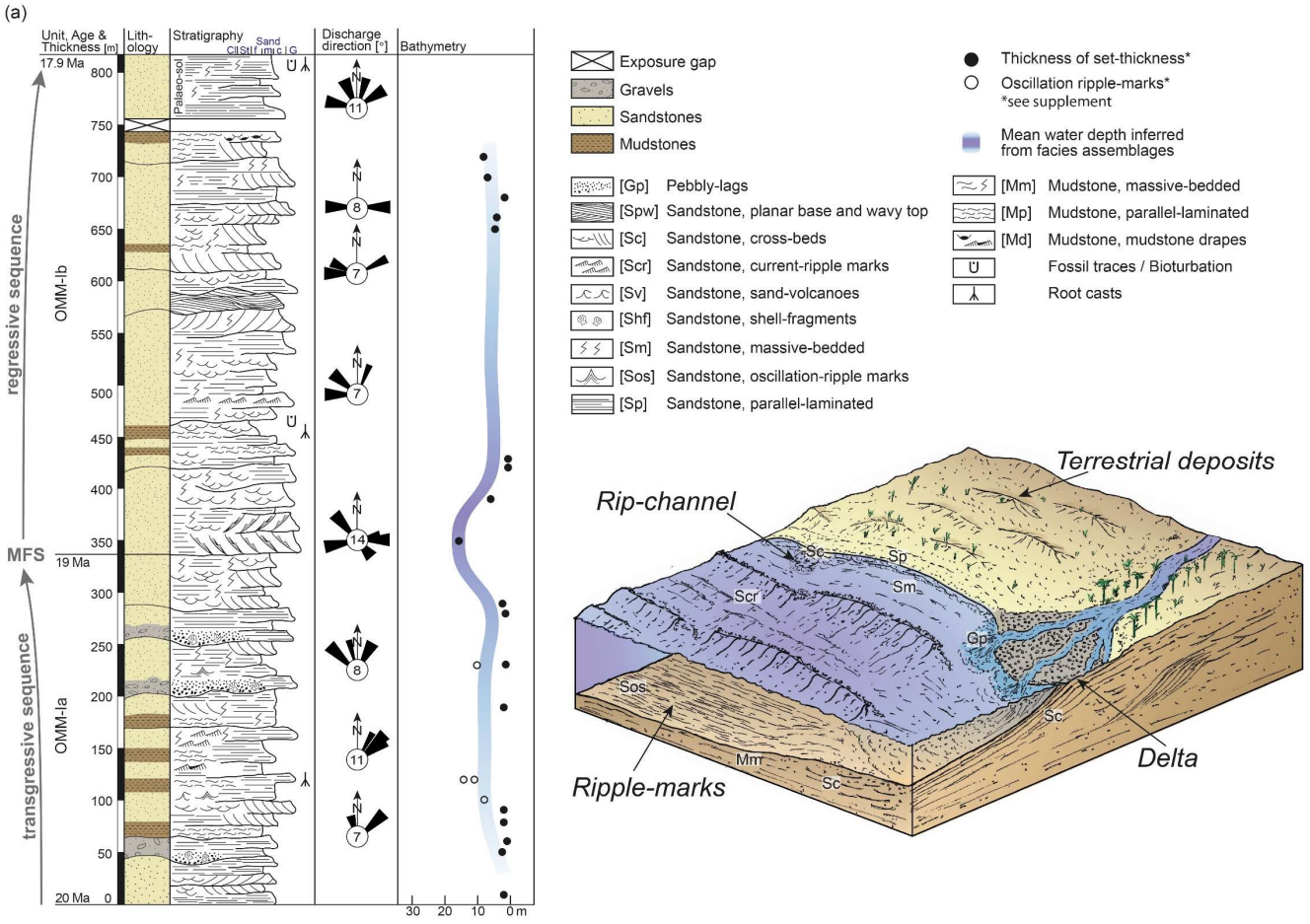
(a)
Unit, Age & Thickness [m]
Lith-ology
Stratigraphy
Sand
Discharge direction [°]
Bathymetry
17.9 Ma
regressive sequence
OMM-Ib
MFS
19 Ma
transgressive sequence
OMM-Ia
20 Ma
Palaeo-sol
30 20 10 0 m
Exposure gap
Gravels
Sandstones
Mudstones
Thickness of set-thickness*
Oscillation ripple-marks*
*see supplement
Mean water depth inferred from facies assemblages
[Gp] Pebbly-lags
[Spw] Sandstone, planar base and wavy top
[Sc] Sandstone, cross-beds
[Scr] Sandstone, current-ripple marks
[Sv] Sandstone, sand-volcanoes
[Shf] Sandstone, shell-fragments
[Sm] Sandstone, massive-bedded
[Sos] Sandstone, oscillation-ripple marks
[Sp] Sandstone, parallel-laminated
[Mm] Mudstone, massive-bedded
[Mp] Mudstone, parallel-laminated
[Md] Mudstone, mudstone drapes
Fossil traces / Bioturbation
Root casts
Terrestrial deposits
Rip-channel
Sc
Sp
Sm
Scr
Gp
Sos
Sc
Mm
Sc
Ripple-marks
Delta

(b)

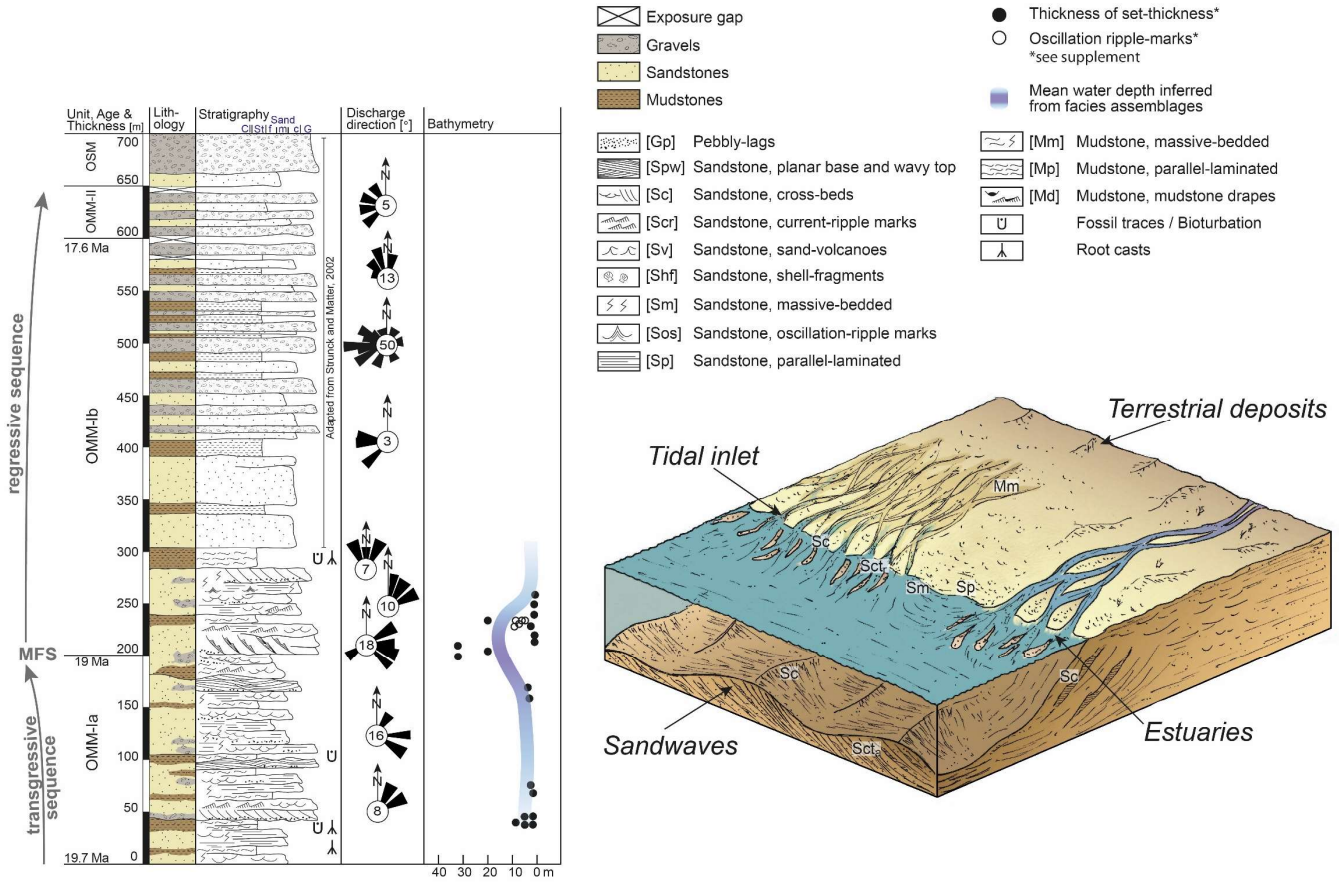

Figure 4: Sedimentological logs of **a)** the Entlen and **b)** the Sense section. See Fig. 2a for locations of sections, Fig. 5 for chronological framework of the deposits and the tables for further sedimentological details and abbreviations of the lithofacies, and for references to sedimentological work. The block-diagrams illustrate the palaeo-geographical conditions from a conceptual point of view. Note that the palaeo-bathymetric values are minimum estimates and that the mean water depths have been inferred from the assignment of lithofacies to depositional environment. This might explain why the numerical values for water-depths based on cross-bed thicknesses and our inferred mean water-depth estimates deviate between c. 200 m and 250 m for the Sense-section.

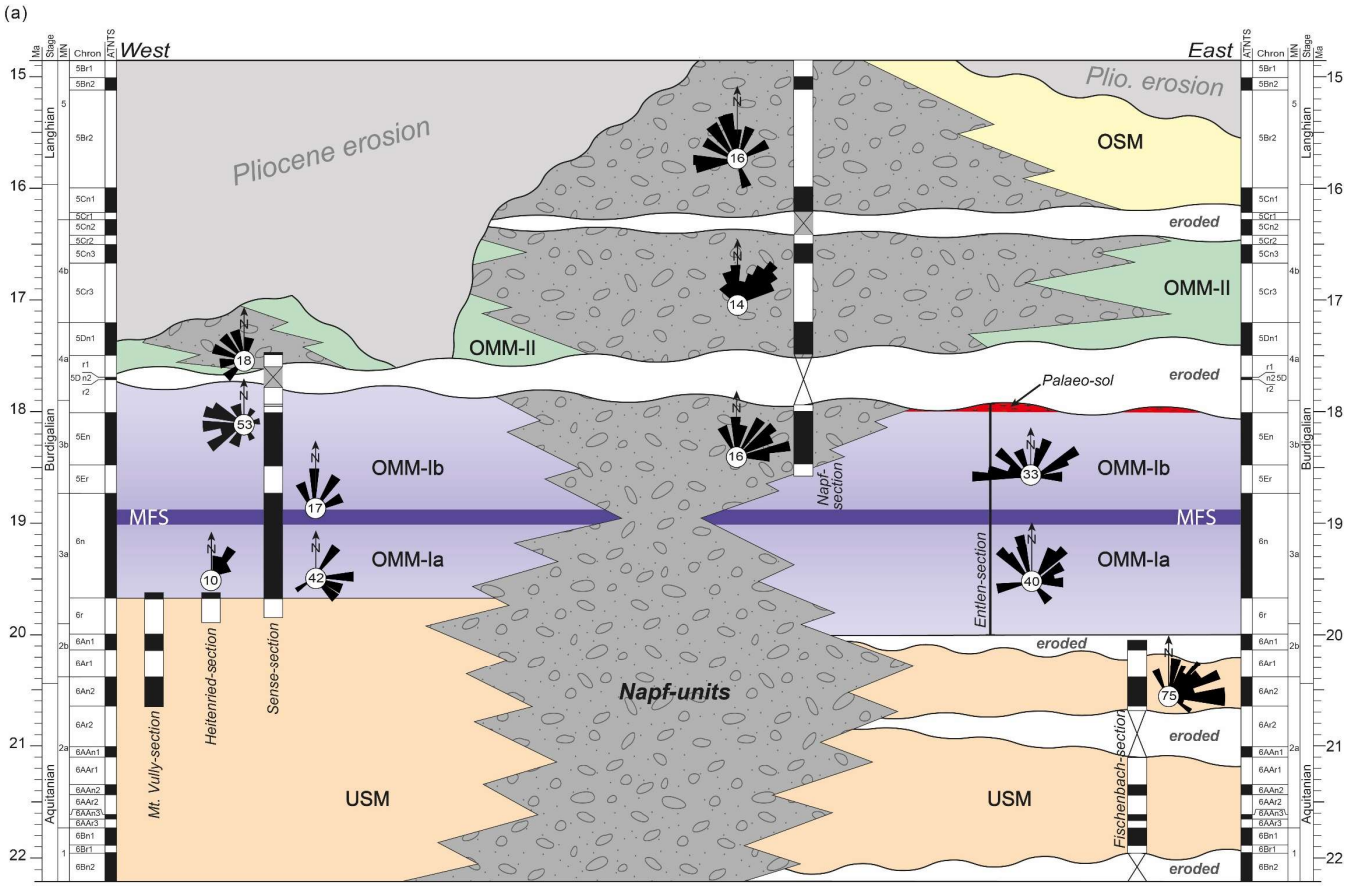
(a)
West
East
Pliocene erosion
Plio. erosion
OSM
OMM-II
OMM-Ib
OMM-Ia
MFS
Napf-units
USM
eroded
Palaeo-sol
Napf-section
Entlen-section
Mt. Vully-section
Heitenried-section
Sense-section
Fischenbach-section
Langhian
Burdigalian
Aquitanian
Chron
Stage
Ma
MN
ATNTS

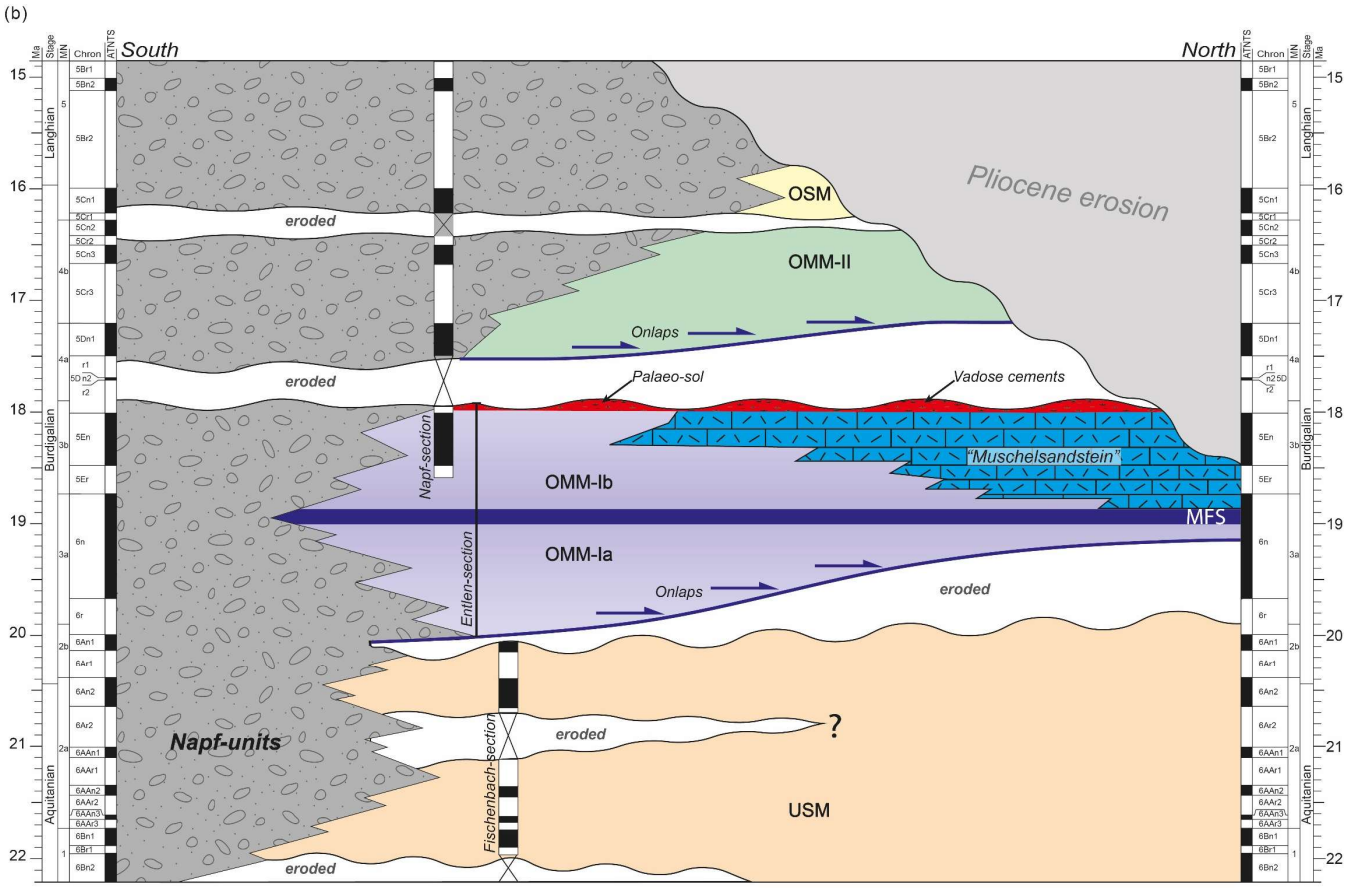

Figure 5: a) West-East chronological (Wheeler) diagram of the Molasse sequence at the proximal basin border between Fribourg and Lucerne (Fig. 2a). The following magnetostratigraphic data have been used: Mt. Vully, Heitenried and Sense (Strunck and Matter, 2002), and Napf and Fischenbach (Schlunegger et al., 1996). Palaeo-transport directions from Heitenried and the upper part of the Sense-section are taken from Strunck and Matter (2002). Note, that the Entlen-section is not calibrated with magnetostratigraphic data but has been adjusted using regional information (see text for further details and Fig. 3b for synthetic sections of the region). MFS = Maximum-flooding surface. Note that Pliocene erosion removed most of the OMM-II record in western Switzerland. We infer marine conditions in the western Swiss Molasse basin during OMM-II times because: (i) marine conditions were present east of the Napf-units, and (ii) material transport occurred towards the west, which implies that marine conditions were also present west of the Napf megafan at that time as confirmed by mapping (e.g., Wanner et al., 2019); **b)** North-South chronological (Wheeler) diagram of the Molasse sequence between Entlen (site 13) and Madiswil (site 14, both on Fig. 2a). See text for further details. The onlaps (blue arrows) are based on interpretations from seismo-stratigraphic data (Schlunegger et al., 1997). MFS = Maximum-flooding surface.

(a)

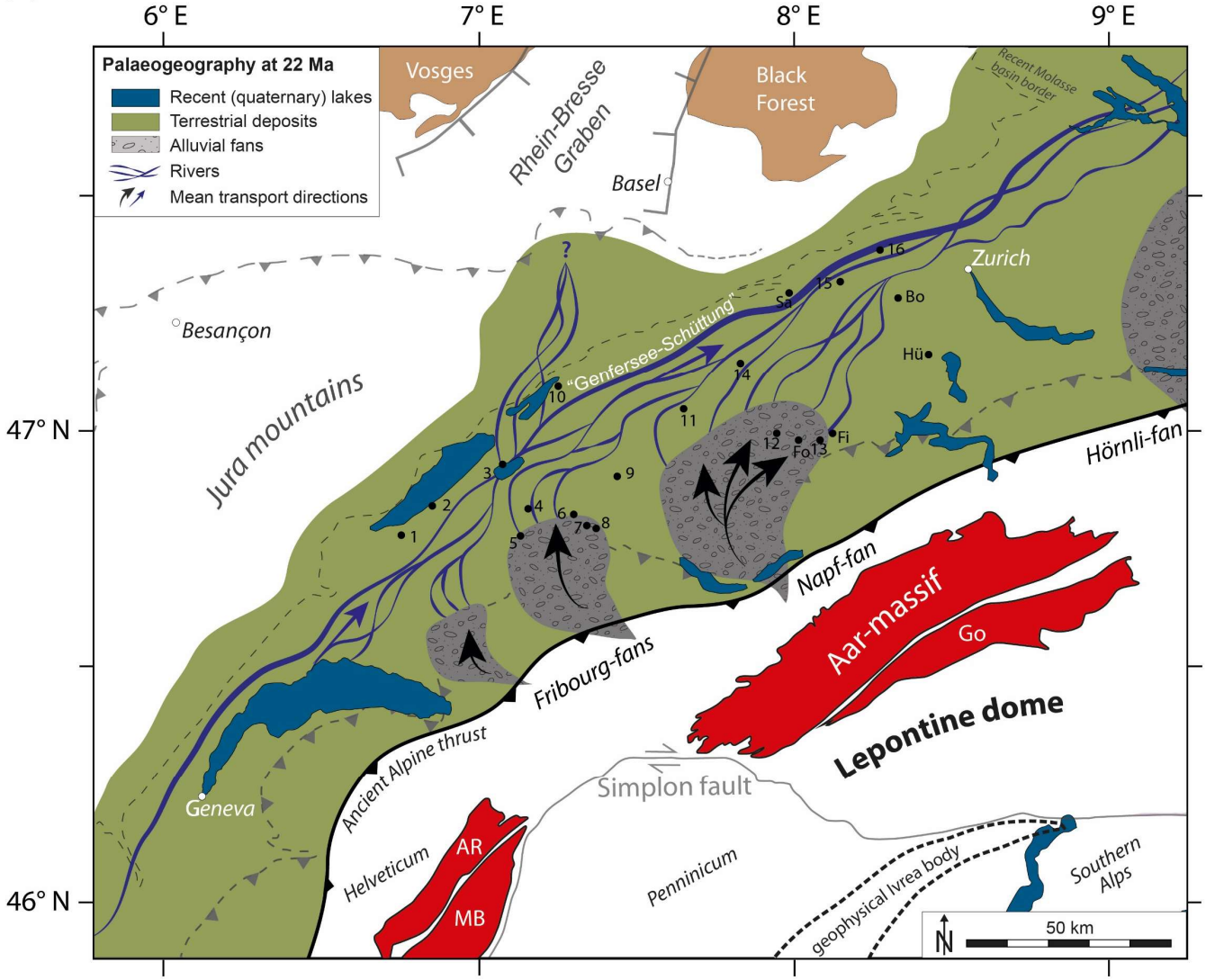
6° E
7° E
8° E
9° E
47° N
46° N
Palaeogeography at 22 Ma
Recent (quaternary) lakes
Terrestrial deposits
Alluvial fans
Rivers
Mean transport directions
Vosges
Rhein-Bresse Graben
Black Forest
Basel
Recent Molasse basin border
Zurich
Besançon
Jura mountains
"Genfersee-Schüttung"
Hörnli-fan
Napf-fan
Aar-massif
Go
Lepontine dome
Fribourg-fans
Ancient Alpine thrust
Simplon fault
Geneva
Helveticum
AR
MB
Penninicum
geophysical Ivrea body
Southern Alps
50 km
N
Bo
Hü
Fo
Fi
Sa

(b)

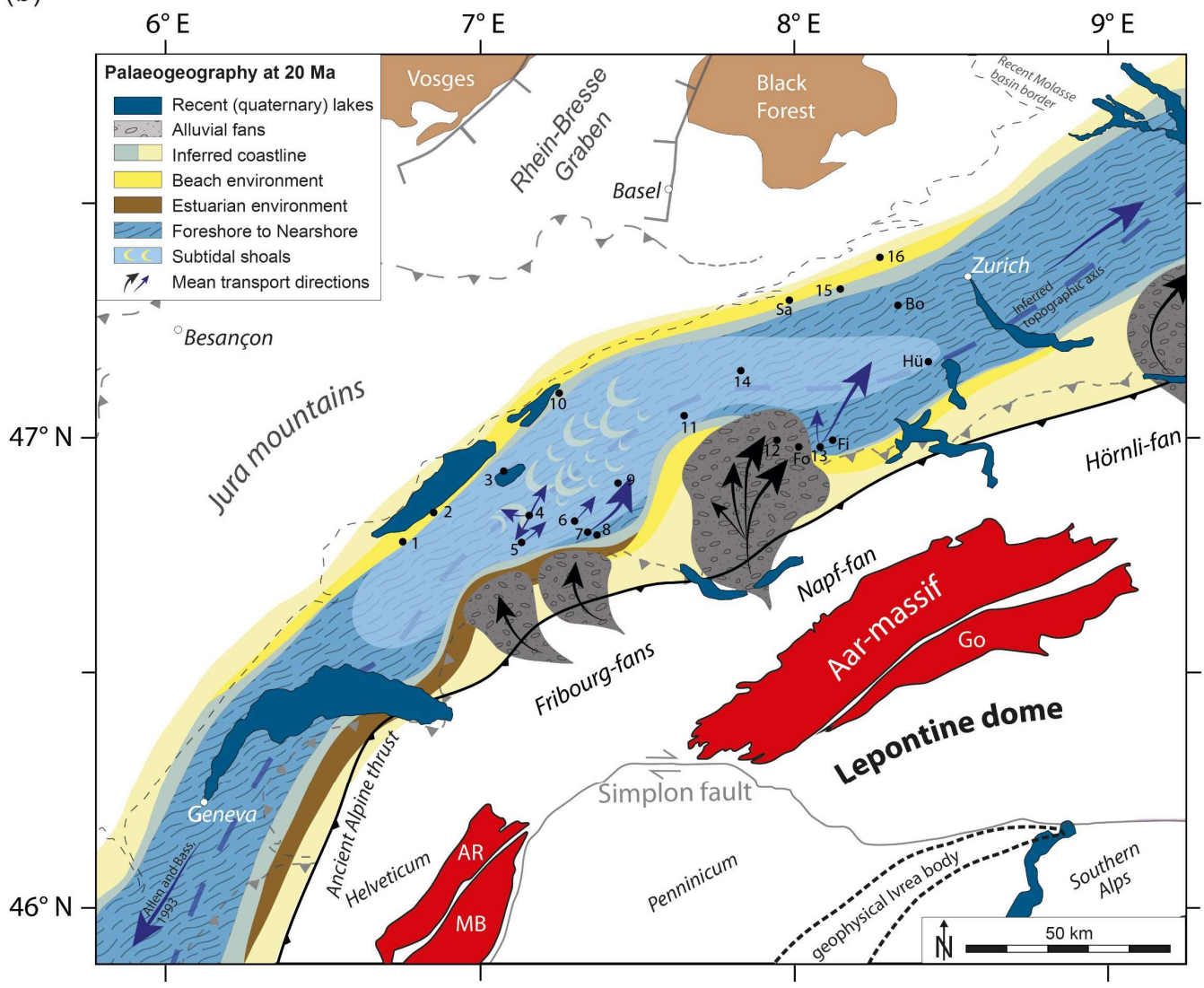
6° E
7° E
8° E
9° E
47° N
46° N
Palaeogeography at 20 Ma
Recent (quaternary) lakes
Alluvial fans
Inferred coastline
Beach environment
Estuarian environment
Foreshore to Nearshore
Subtidal shoals
Mean transport directions
Vosges
Rhein-Bresse Graben
Black Forest
Basel
Recent Molasse basin border
Zurich
Inferred topographic axis
Besançon
Jura mountains
Hörnli-fan
Napf-fan
Aar-massif
Go
Lepontine dome
Fribourg-fans
Simplon fault
Ancient Alpine thrust
Helveticum
AR
MB
Penninicum
Geneva
Allen and Bass, 1993
geophysical Ivrea body
Southern Alps
50 km
Sa
Bo
Hü
Fi
Fo
1
2
3
4
5
6
7
8
9
10
11
12
13
14
15
16

5

(c)

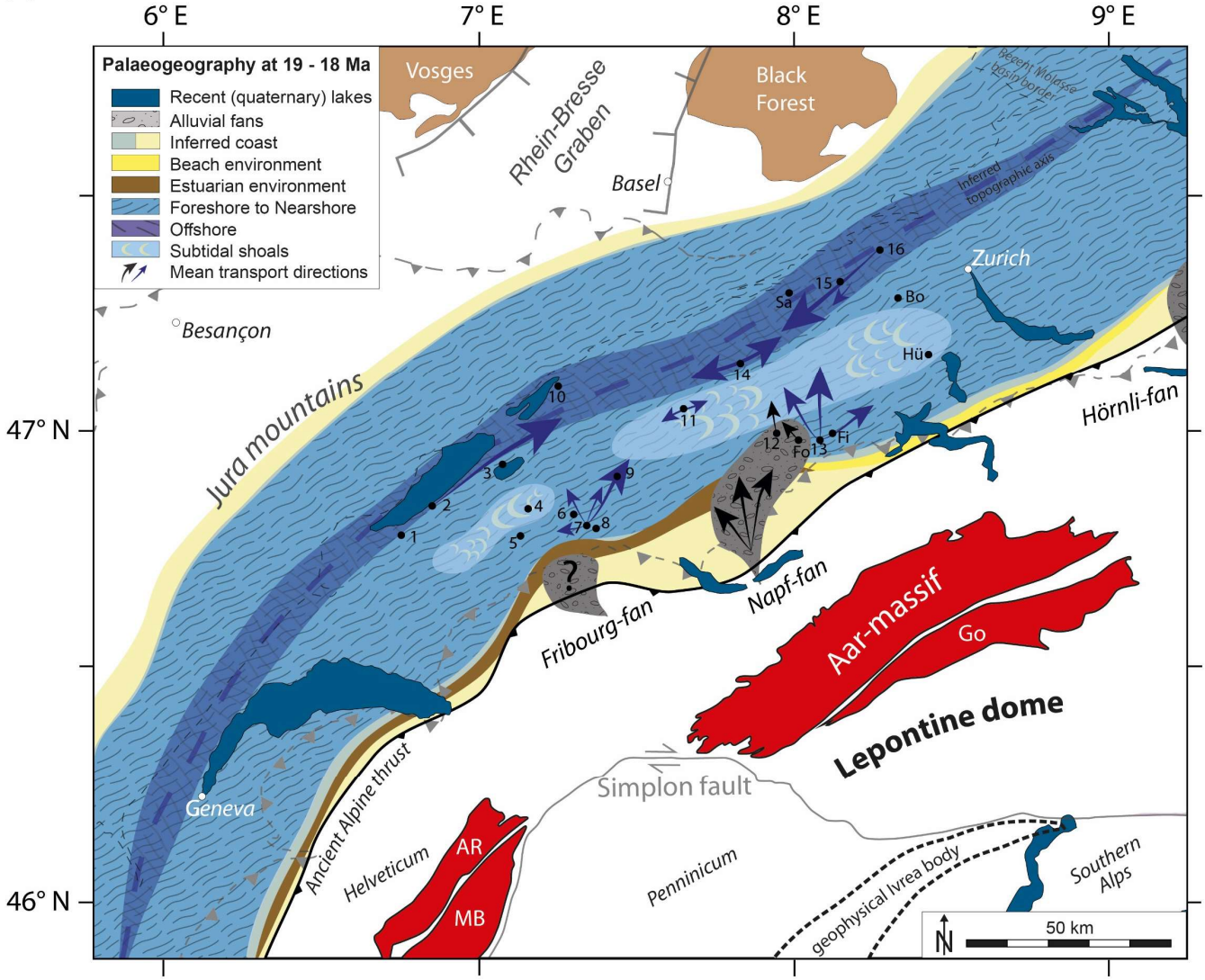
Palaeogeography at 19 - 18 Ma
Recent (quaternary) lakes
Alluvial fans
Inferred coast
Beach environment
Estuarian environment
Foreshore to Nearshore
Offshore
Subtidal shoals
Mean transport directions
6° E
7° E
8° E
9° E
47° N
46° N
Vosges
Rhein-Bresse Graben
Black Forest
Basel
Besançon
Zurich
Jura mountains
Hörnli-fan
Napf-fan
Fribourg-fan
Aar-massif
Go
Lepontine dome
Simplon fault
Ancient Alpine thrust
Helveticum
AR
MB
Penninicum
geophysical Ivrea body
Southern Alps
Geneva
inferred topographic axis
50 km
N
Sa
Bo
Hü
Fo
Fi

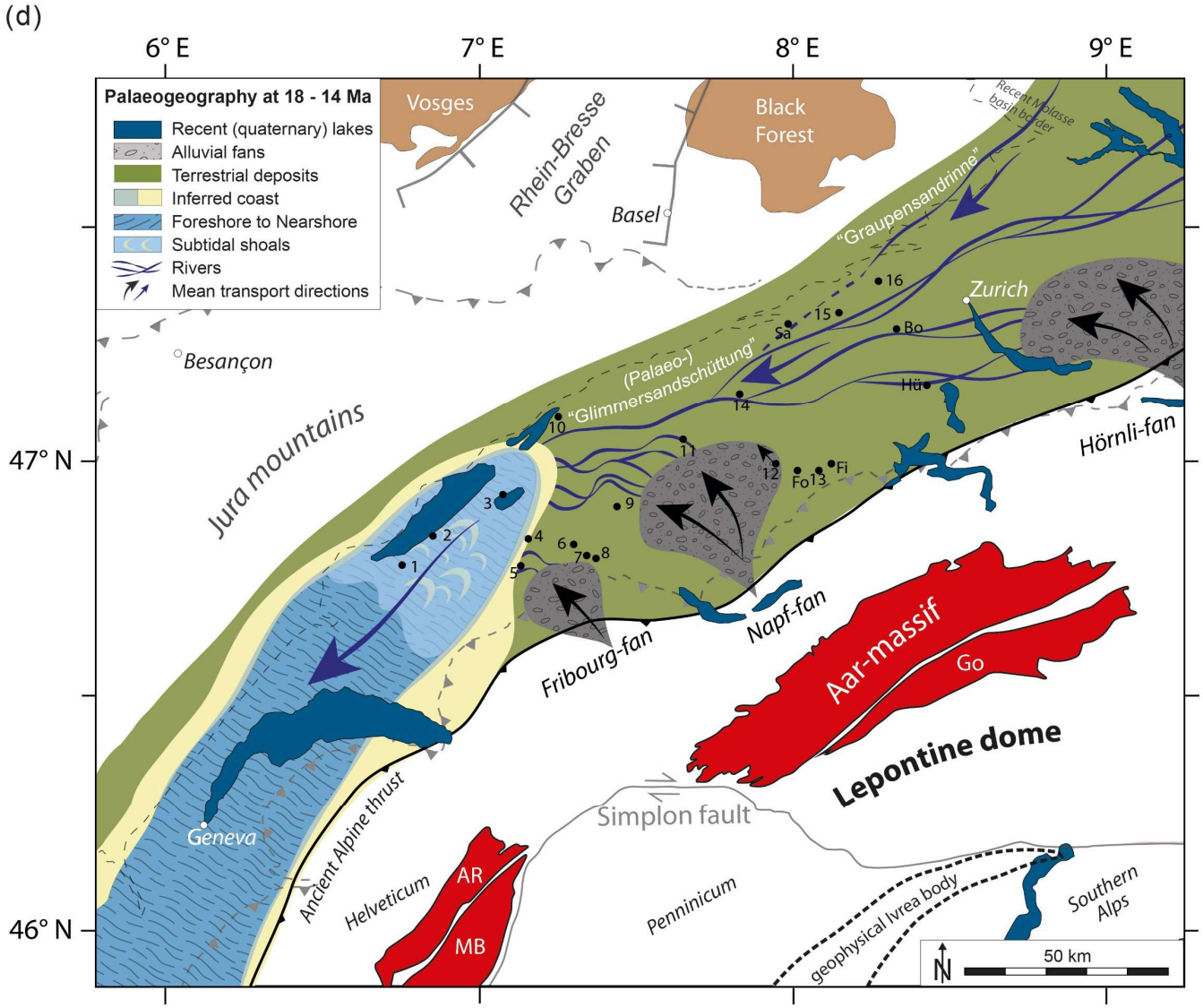

Figure 6: Palaeogeographical reconstructions of the Molasse basin at different stages: **a)** USM (c. 22 Ma), **b)** OMM-Ia (c. 20 Ma), **c)** OMM-Ib (c. 19-18 Ma) and **d)** OMM-II to OSM (c. 18- 14 Ma) modified after Kuhlemann and Kempf (2002) based on own observations Note that all maps show present-day lithotectonic units within the Alps and the Jura mountains for orientation purposes (dashed lines and grey-coloured lines). We acknowledge that the positions of these and the surface patterns (such as lakes) were different during deposition of the Molasse deposits. The location of the palaeo-thrust fronts (thick line) are adapted from Kuhlemann and Kempf (2002). Black dots mark study sites for orientation purposes. Please refer to Fig. 1 for the complete legend.

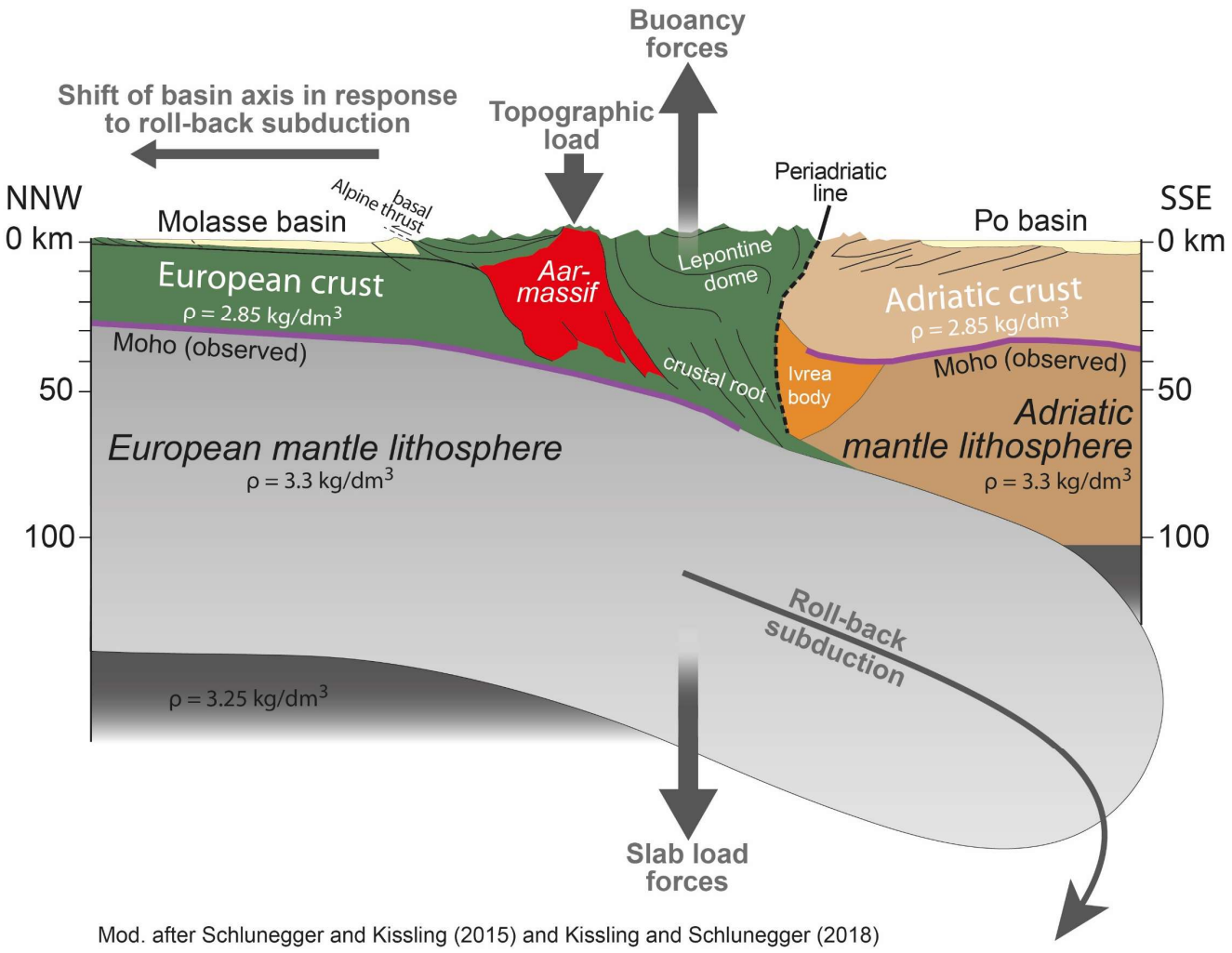

Figure 7: Simplified geological-geophysical model of the Alpine orogen for the time between 20-18 Ma, showing the most important geodynamic forces that might have shaped the Molasse basin. Modified after Schlunegger and Kissling (2015) and Kissling and Schlunegger (2018).

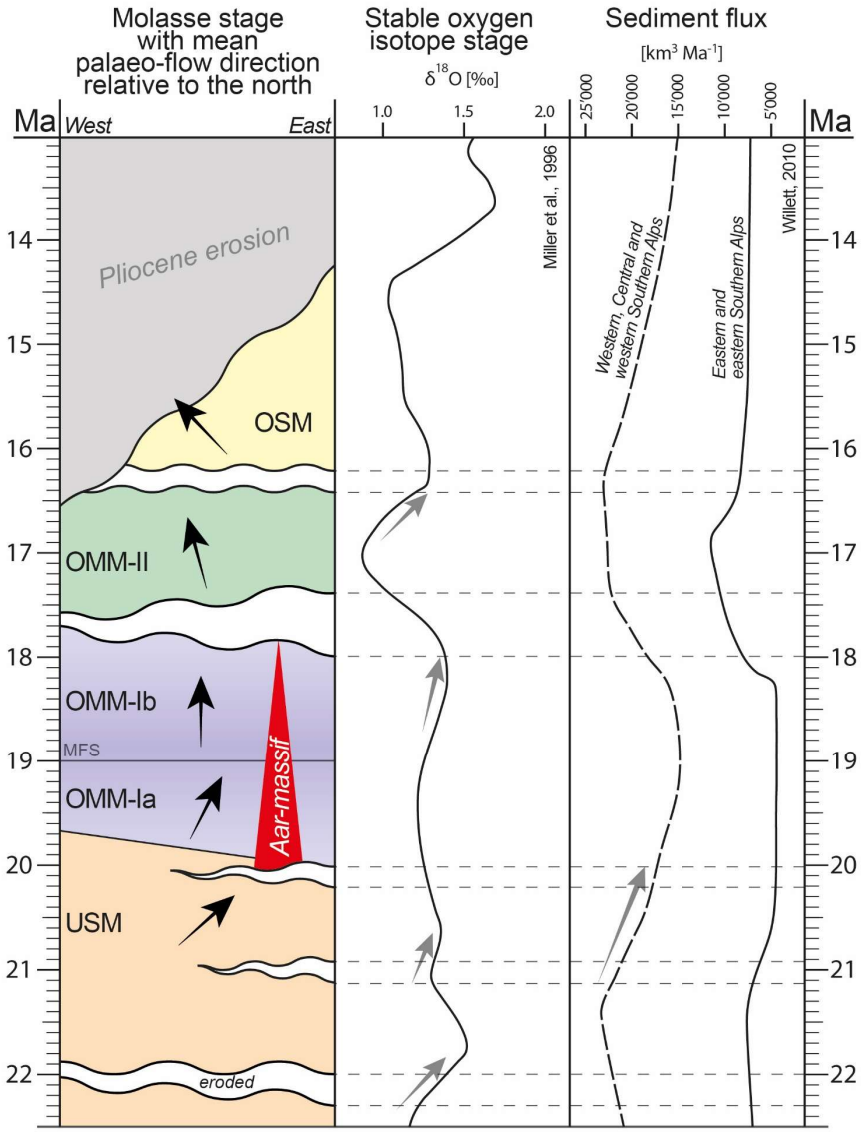

Figure 8: Molasse stages (USM, OMM and OSM) with mean palaeo-transport directions (black arrows), hiatuses plotted against stable oxygen isotope stages (Miller et al., 1996) and sediment flux (Kuhlemann, 2000; Willet, 2010). The red triangle demarcates the onset of delamination and rapid exhumation of the Aar-massif (Herwegh et al., 2017). Grey arrows demarcate falls in sea level and decreases in sediment flux possibly contributing to the related hiatuses. MFS = Maximum-flooding surface.